A three-stage decision-making process for cost-effective passive solutions in office buildings in the hot summer and cold winter zone in China

Article

Accepted Version

Cao, X., Wang, K., Xia, L., Yu, W., Li, B., Yao, J. and Yao, R. ORCID: https://orcid.org/0000-0003-4269-7224 (2022) A three-stage decision-making process for cost-effective passive solutions in office buildings in the hot summer and cold winter zone in China. Energy and Buildings, 268. 112173. ISSN 1872-6178 doi: https://doi.org/10.1016/j.enbuild.2022.112173 Available at https://centaur.reading.ac.uk/106131/

To link to this article DOI: http://dx.doi.org/10.1016/j.enbuild.2022.112173

Publisher: Elsevier

A three-stage decision-making process for cost-effective passive solutions in office buildings in the Hot Summer and Cold Winter zone in China

Xinyun Cao[a,b], Kaixuan Wang[a,b], Lin Xia[d], Wei Yu[a,b], Baizhan Li[a,b], Jinyang Yao[e], Runming Yao[a,c*],

a Joint International Research Laboratory of Green Buildings and Built Environments (Ministry of Education), Chongqing University, Chongqing, 400045, China

b National Centre for International Research of Low-carbon and Green Buildings (Ministry of Science and Technology), Chongqing University, Chongqing, 400045, China

c School of the Built Environment, University of Reading, Reading, RG6 6DF, UK

d East China Architectural Design & Research Institute Co., Ltd，Shanghai, 200032, China

e University of British Columbia, BC, V6T 1Z4, Canada

*Corresponding authors:

Runming Yao, E-mail addresses: r.yao@cqu.edu.cn; r.yao@reading.ac.uk

Abstract

China, with the largest energy consumption system in the world, faces numerous challenges in achieving the government's commitment to reach a carbon-peak and carbon-neutral target. As the most common public building type in terms of floor area, office buildings have great potential for energy saving and emissions reduction. To meet this target, building designers target passive solutions that can meet the thermal comfort needs of occupants and also reduce energy consumption. This study aims to develop a decision-making method to select optimal solutions from among tens of thousands of design options considering the factors of energy consumption, comfort, and cost. We developed a novel optimization decision approach with the above-mentioned three objectives. The model consists of three stages: 1) the establishment of the reference building model, 2) sensitivity analysis to identify the main influencing variables, and 3) the establishment of the optimization and decision-making model by applying NSGA-II and TOPSIS methods. By applying this three-stage decision-making model, this paper first proposes cost-effective passive design solutions for office buildings throughout the Hot Summer and Cold Winter climate zone.

Finally, an office building in Shanghai was chosen as a case study to demonstrate the practical implementation of the proposed solutions through a post-occupancy evaluation with a two-year energy auditing and thermal comfort survey. It is evident that the proposed solutions provide support for the new low energy building design guide for office buildings along with necessary revisions to the existing standards for the hot summer and cold winter climate zone in China.

Keywords

office buildings, cost-effective passive solutions, multi-objective optimization, decision-making, Hot Summer and Cold Winter

Acronyms

aPMV	Adaptive Predicted Mean Vote
ANN	Artificial Neural Network
BEO	Building Energy Optimization
CDD	Cooling Degree Days
COP	Coefficient of Performance for heating [W/W]
EER	Energy Efficiency Ratio for cooling [W/W]
$EUI_{H\&C}$	Annual Energy Use Intensity for heating and cooling [kWh/ m^2]
GA	Genetic Algorithm
HSCW	The Hot Summer and Cold Winter climate zone
HVAC	Heating, Ventilation, and Air Conditioning
HDD	Heating Degree Days
LCC	Life Cycle Cost
NSGA-II	Non-dominated Sorting Genetic Algorithm II
PMV	Predicted Mean Vote
SHGC	Solar Heat Gain Coefficient of the Window
TOPSIS	Technique for Order of Preference by Similarity to the Ideal Solution
WWR	Window-to-Wall Ratio
XPS	Extruded Polystyrene

1 Introduction

1.1 Background information

In response to global climate change, China has set ambitious carbon emission targets to reach its carbon peak by 2030 and to be carbon neutral by 2060. The building sector, as one of the major energy-consuming sectors, accounted for more than 42% of total carbon emissions in 2018 [1] and is the most important sector for energy saving and emissions reduction. Public buildings play a pivotal function in China's economic, social, and cultural development. The total area of public buildings in China had reached 12.8 billion m^2 in 2018 [1] and office buildings account for nearly 30% of the total energy consumption of public and commercial buildings in China [2].

The current energy efficiency standards for office buildings can be divided into two categories: mandatory standards and recommended standards. All new buildings should follow the design provisions of the mandatory standards. The current mandatory standard is 'Design standard for energy efficiency of public buildings (GB50189-2015)', which was released in 2015, and this standard needs to be revised as people's comfort level increases and new carbon emission reduction targets are set. The other category is the recommended standards, such as the 'Zero Energy Building Technology Standard (GBT 51350-2019)', which mainly aims at reducing building energy consumption and guiding new buildings to implement strict building technology design indexes, but the higher incremental costs of Zero Energy Buildings have become a barrier to property developers [3, 4]. There is an urgent need to explore technical solutions and standards that both reduce energy consumption and consider the occupants' comfort whilst taking into account cost.

The Hot Summer and Cold Winter climate zone (HSCW) is a densely populated area with the fastest economic development in China. Its climate is unique, the summers are hot and long and winters are cold and humid [5] leading to both high cooling and heating demands. Therefore, the energy consumption for heating and cooling is an important part of the office buildings' operational energy consumption. A government report has published the electricity consumption of 610 office buildings and 206 government office buildings in Shanghai showing that the Energy Use Intensity for heating and cooling ($EUI_{H\&C}$) of public buildings accounted for 28.5% of the total electricity consumption in 2019 [6]. The Chongqing Building Technology Development Center conducted a study on office buildings and the proportion of $EUI_{H\&C}$ to the total energy consumption was about 50.7%. Zhu *et al.* [7] conducted a study on 21 office buildings of government departments in Hangzhou, and the results showed that the $EUI_{H\&C}$ accounted for about 33% of the total building energy consumption. In summary, reducing $EUI_{H\&C}$ is one of the priorities of building energy conservation.

1.2 Existing studies

Building passive design technologies related to $EUI_{H\&C}$ include envelope thermal performance, shading, and ventilation strategies. In response to the climatic characteristics of hot and humid regions, numerous scholars have conducted studies on the adaptability of various building energy efficiency technologies. Some typical studies are listed in Table 1. These studies mainly include 1) research on the optimal thickness of building envelope insulation materials [8-11], 2) exploration of suitable parameters for building exterior window performance [12-14], 3) research on shading strategies [12, 15], 4) research on building natural ventilation strategies [16], and 5) analysis of new envelope technologies or materials [17]. These explorations on the climate suitability of individual technologies provide strong support to optimize the building design.

However, the impact of various technologies on $EUI_{H\&C}$ is complex. A single technology does not bring out the best potential for building energy efficiency. How to optimize the design of multiple energy-saving technologies to achieve design goals is a key issue. Some scholars have set up different design scenarios to explore the best combination of multiple technologies in the HSCW zone using the traditional one-by-one simulation method. Yao *et al.* [18] analyzed the effect of passive design measures on $EUI_{H\&C}$ and thermal comfort in the HSCW zone, such as building orientation, thermal insulation, glazing area, shading devices, air tightness, and natural ventilation. Ge *et al.* [19] worked out the energy efficiency optimization strategies in terms of building envelope thermal performance, sun shading, and adaptive space heating and cooling behavior in research office buildings in Hangzhou.

When more technologies are available, there can be tens of thousands of design solutions. Multi-objective optimization algorithms can quickly find the solution set that satisfies the objectives among many solutions. Farshad Kheiri [20] summarized the application of algorithms for multi-objective optimization in recent years and pointed out that the application rate of the genetic algorithm (GA) has increased rapidly since 2000 and is much higher than other methods. Bichiou *et al.* [21] compared and analyzed three optimization algorithms, GA, Particle Swarm and Sequential Search, and concluded that GA is the algorithm with the shortest computer runtime to achieve the objective. In the process of specific research applications, GA has been studied and improved by a large number of researchers. Deb [22], an Indian scholar, improved GA and proposed the non-dominated and crowding distance sorting genetic algorithm (NSGA-II), which improved the optimization speed and accuracy of the traditional GA. To quickly and accurately obtain the optimal building design solution, some scholars have combined building energy simulation software with intelligent optimization algorithms to find the optimal combination of building design parameters that meet the objectives [23, 24]. Some typical studies in the HSCW zone have been listed in Table 1. Gou *et al.* [25] developed a double-objective optimization model to optimize the passive design of newly-built residential buildings, using the NSGA-II coupled with the Artificial Neural Network (ANN) in Shanghai. Taking residential buildings in Chongqing as research subjects, Yu *et al.* [26] established a residential model with the double objectives of optimizing $EUI_{H\&C}$ and comfort , where 14 main building design parameters were selected as the design variables of the optimization model, and the optimal Pareto solution set was obtained. Zhao *et al.* [27] conducted a multi-objective optimization design for office buildings in different climate zones in China, aiming to minimize the heating, cooling, and lighting energy consumption and discomfort hours.

Table 1 Summary of the studies focused on building design passive measures in hot and humid regions

Authors	Areas	Building types	Methodology	Objectives	Technologies	Main findings
Dutta *et al.* [15]	Tropical climate	Commercial hospital building	TRNSYS simulation software	Heating and cooling energy consumption	Shading device	An automated experimentally designed movable exterior window shading device linked with the sun path is proposed. Incorporation of movable shading devices can reduce energy consumption by 9.8%.
Ghosh *et al.* [12]	Warm and humid climate	Not mentioned	EnergyPlus simulation software	Heating, cooling and lighting energy consumption	Window to wall ratio (WWR) and shading	● When the WWR increases from 13.33% to 53.33%, the total energy consumption increases by 26.67%; ● Compared to the window with no shading device, the total energy consumption was reduced by 4.62% for the newly designed shading.
Marino *et al.* [13]	12 weather conditions in Italy	Office building	EnergyPlus simulation software	Heating, cooling and lighting energy consumption	WWR	● The optimal value of WWR is slightly influenced by climate conditions. ● The average WWR values are 23.5% for the least insulated building and are 25.9% for the most insulated building.
Lee *et al.* [14]	5 typical Asian climates	Office building	EnergyPlus simulation software	Heating, cooling and lighting energy consumption	Window properties	● The value of WWR is recommended lower than 25%. ● Triple glazing offers a performance advantage in saving heating energy in all climates.
Taleb *et al.* [28]	The hot climate of Dubai	Residential buildings	IES and CFD simulation software	Cooling energy consumption	Natural ventilation	The correct combination of active cooling systems and natural ventilation strategies has the potential to reduce the cooling energy consumption by 25%.
Mottet *et al.* [16]	Chongqing and Hangzhou, the HSCW zone, China	Residential buildings	EnergyPlus and CFD simulation software	Thermal comfort condition	Natural ventilation	Two ventilation solutions have been proposed to reduce the indoor temperature of typical two-bedroom study flats.
Yao *et al.* [18]	Chongqing, the HSCW zone, China	Residential building	EnergyPlus simulation software	$EUI_{H\&C}$ and thermal comfort condition	Building orientation, thermal insulation, glazing area, shading devices, air tightness, and natural ventilation	An extensive parametric analysis of several passive strategies was carried out for a typical apartment block located in the HSCW zone.
Ge *et al.* [19]	Hangzhou, the HSCW zone, China	University research building	EnergyPlus simulation software	$EUI_{H\&C}$ and thermal comfort condition	Building envelope thermal performance, shading, and human	In the analysis of investigated, measured and simulated data, typical adaptive behaviors and energy efficiency optimization strategies are analyzed.

					behavior	
Chen *et al.* [29]	Singapore	Office building	NSGA-II	Cooling energy consumption, Daylighting	WWR, shading strategy, glazing material	A double-objective optimization model is developed and the optimization result is manually clustered and compared.
Gou *et al.* [25]	Shanghai, the HSCW zone, China	Residential building	NSGA-II Artificial Neural Network (ANN)	Building Energy Demand, Comfort Time Ratio	17 main building design parameters	A double-objective optimization model is developed to optimize the passive design of newly-built residential buildings.
Yu *et al.* [26]	Chongqing，the HSCW zone, China	Residential building	Back Propagation Neural Network (GA-BP), NSGA-II, EnergyPlus simulation software	$EUI_{H\&C}$ and thermal comfort condition	14 main building design parameters	A model with the double objectives of optimizing $EUI_{H\&C}$ and comfort was established.
Zhao *et al.* [27]	5 climatic regions, China	Office building	NSGA-II, DesignBuilder simulation software	Heating, cooling, and lighting energy consumption and discomfort hours	Building orientation, the configuration of windows and shading system	A set of Pareto solutions are obtained after optimization, which can give designers different scheme choices based on preferences.

126

1.3 Research gaps and contributions

The above analysis of existing studies reveals two main research gaps in building design optimization. First and foremost, previous studies lack the critical step of conducting further decision-making processes to obtain an optimal solution from the Pareto solution set. Building designers still face the challenge of making decisions on the best solution among many candidate solutions. Furthermore, there are few studies of cost-effective design solutions for office buildings in the HSCW climate zone. Architects play important roles in the decision-making affecting building design solutions. However, the optimization processes are complex and time-consuming. The lack of a robust approach supporting an architect becomes a hurdle for the delivery of low energy building designs which is particularly important at the early design stage.

To fill these research gaps, this study aims to develop a decision-making model to obtain cost-effective design solutions for office buildings in the HSCW climate zone. The research results will provide a solid reference for the building designers and the revision of energy efficiency design standards for office buildings in the HSCW region.

2 Methodology

2.1 Framework

This study attempts to propose a decision-making model for cost-effective solutions for office buildings in the HSCW zone. To obtain solutions with high generalizability, it is crucial to select a reference building that reflects the main physical and thermal characteristics of most office buildings. The first stage of the model is to identify a representative reference building. The sensitivity analysis method identifies the key factors affecting the research objectives and reduces the input parameters for the optimization model. The second stage is a key step to improve the efficiency of the optimization model and to analyze the rationality of the final solutions. Cost-effective office building design solutions are those that provide a comfortable indoor environment, are economically feasible, and have low energy consumption. Therefore, the decision-making process conducted in the third stage is analyzed with comfort, energy and cost as the three objectives. To verify the feasibility of the decision-making process and solutions proposed in this paper, an office project located in the A2 climate sub-zone was finally selected as a research case for this study. This is analyzed from two perspectives: objective parameter testing and a subjective survey of the occupants. Two years of monitored data and a questionnaire survey of occupants were used to verify the practical effectiveness of the proposed solutions. Figure 1 shows the research methodology framework.

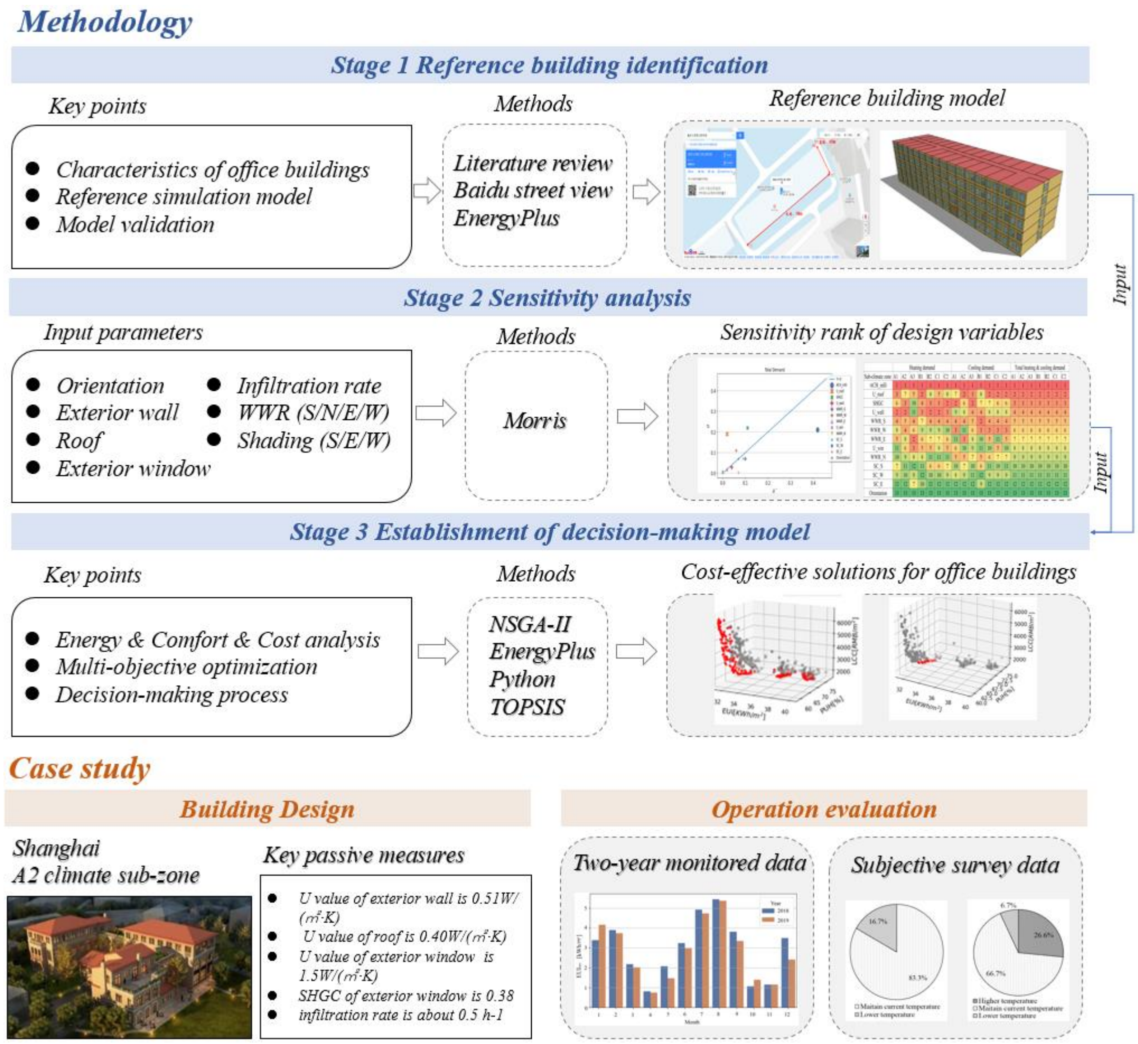

Figure 1: Framework of this research

The three stages of the decision-making model are described in detail as follows:

Stage 1: Identification of the reference building

Seven typical cities are selected from seven climate sub-zones in the HSCW zone, and the office buildings in each typical city are researched to collect characteristic information. Based on these results, a reference building simulation model is established.

Stage 2: Global sensitivity analysis

The Morris global sensitivity analysis method is used to rank the importance of design parameters affecting building energy consumption. Based on the results of the sensitivity analysis, the important design parameters are selected as input variables for the optimization model, thus reducing the number of variables involved in the optimization and shortening the optimization run time.

Stage 3: Establishment of a decision-making model

This stage contains two processes: a multi-objective optimization process and a multi-criteria decision-making process. In the first process, three objectives are defined and the optimization algorithm NSGA-II is applied in this study to obtain Pareto solution sets that meet the three objectives. EnergyPlus is used to simulate energy consumption for heating and cooling and discomfort hours. The Life Cycle Cost (LCC) method is applied to calculate the cost of each solution. The optimization is implemented on the Python platform. In the second process, the TOPSIS decision-making method is applied to rank the alternative solutions from the Pareto solution sets. This helps decision-makers identify the best solutions.

The cost-effective solutions for office buildings in seven sub-zones of the HSCW climate zone are worked out by applying the decision-making model. Finally, a case office building is studied. We comprehensively evaluate the rationality of the case building design solution from two perspectives: objective monitoring and subjective evaluation. Monitored data for energy consumption, indoor air temperature, and indoor air relative humidity were collected over two years and a survey of the occupant's subjective evaluation of indoor thermal conditions was conducted.

2.2 Climate condition of typical cities

The HSCW climate zone is located in the central part of China, which is also called a 'transitional area'[30]. The climate in this area is severe heat in summer and cold in winter. The temperature, humidity, and solar radiation in the entire region vary greatly, so different cities' cooling and heating demand are quite different. Therefore, it is necessary to subdivide this region into several climate sub-zones. Xiong *et al.* [31] performed a cluster analysis of the daily meteorological data from 166 meteorological stations (2006-2015) in the HSCW climate zone for the past 10 years and divided this zone into seven climate sub-zones and selected a typical city for each of them. The climatic characteristics of these typical cities are shown in Table 2 and Figure 2.

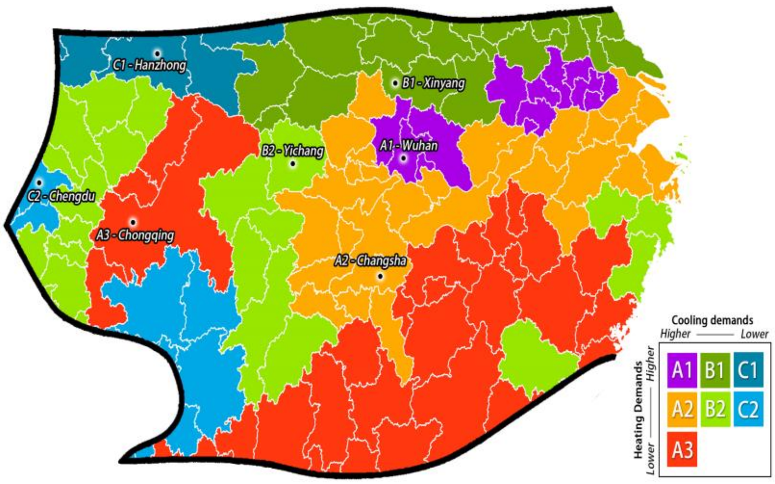

Figure 2: The mapping of seven climate sub-zones in HSCW zone [31]

Table 2: Climatic characteristics of seven typical cities in the HSCW zone

NO.	Climate sub-zone	Typical cities	Cooling demand	Heating demand	HDD18	CDD26
1	A1	Wuhan	High	High	1501	283
2	A2	Changsha	High	Medium	1466	230
3	A3	Chongqing	High	Low	1089	217
4	B1	Xinyang	Medium	High	1863	137
5	B2	Yichang	Medium	Medium	1437	159
6	C1	Hanzhong	Low	High	1945	63
7	C2	Chengdu	Low	Medium	1344	56

As shown in Figure 2, the A1 climate sub-zone is located in the middle of the HSCW zone. Wuhan in the A1 climate sub-zone has the highest total heating and cooling demand and the highest value of CDD26. Both Changsha (A2 climate sub-zone), and Chongqing(A3 climate sub-zone) have high cooling demand, but the two cities have different heating demands, with Changsha's heating demand being higher than that of Chongqing. The B1 climate sub-zone is located in the northern part of the HSCW zone, where the heating demand is high and the cooling demand is medium, and the typical city in this zone, Xinyang, has the highest value of HDD18. Yichang, located in the B2 climate sub-zone, has medium heating and cooling demand. The C1 climate sub-zone is located in the northwestern part of the HSCW zone, where the typical city of Hanzhong has high heating and low cooling demands. The C2 climate sub-zone is located in the western part of the HSCW zone, which has a medium heating demand and the lowest cooling demand making it the mildest climate sub-zone.

In the HSCW zone, the summers are very hot and humid and the winters are very cold and wet. As shown in Figure 3, in summer, the outdoor dry bulb temperature in Wuhan (A1) is the highest, with an average outdoor dry bulb temperature of 30°C in July and a maximum near 39°C. In winter, the outdoor dry bulb temperature in Hanzhong (C2) is the lowest, with an average outdoor dry bulb temperature of 2°C in January and a minimum near -4°C. The average outdoor relative humidity in each city exceeded 70% both in winter and summer. The average solar direct radiation intensity in all cities is over 100W/ m^2 in summer, which means the application of shading devices will provide better energy-saving potential.

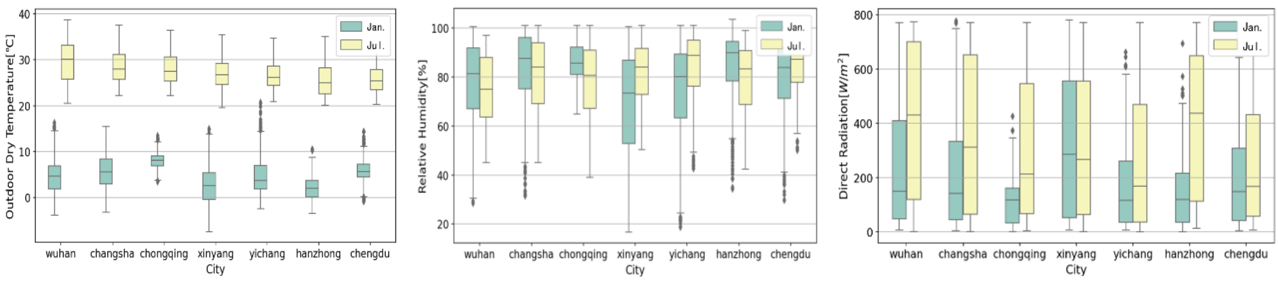

Figure 3: Outdoor climate conditions of the hottest month and coldest month in seven cities

2.3 Model setting of the reference building

The selection of the reference building determines whether the research results are representative**.** At present, the model of a typical office building has not been established in the HSCW zone. Therefore, in this study, the basic characteristic information of office buildings is investigated using Baidu map street view information in the HSCW zone. The main research architecture shape information includes length, width, and the number of floors. The length and width data of the building are directly measured through the measurement tool that comes with Baidu Maps, and the numbers of floors of the building are obtained using street view data. This method can greatly help in obtaining building information on a large scale without a large labor cost compared with the traditional ground survey method. The limitation of the method though is that a few buildings are obscured by surrounding buildings, trees, etc. and some information cannot be obtained accurately. However, the missing information can be obtained through photos or descriptions of the buildings on websites.

A total of 217 office buildings were investigated in seven typical cities, including 20 buildings in Wuhan (A1), 50 buildings in Changsha (A2), 55 buildings in Chongqing (A3), 18 buildings in Xinyang (B1), 21 buildings in Yichang (B2), 15 buildings in Hanzhong (C1), and 38 buildings in Chengdu (C2).

The main building shape information of these buildings was obtained through Baidu map, including the length, width, number of floors, and height of each building. The survey results are shown in Figure 4, the length of most offices ranges from 56 to 82m, the width ranges from 15 to 35m, the height ranges from 16 to 32m, and the number of floors ranges from 4 to 8.

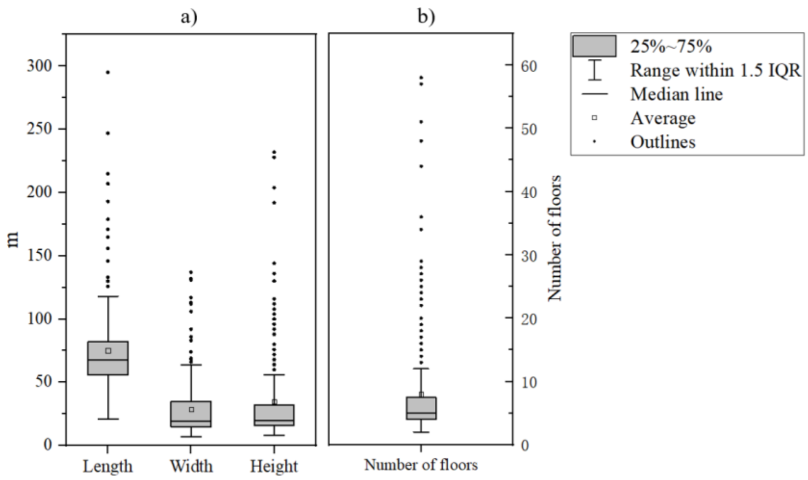

Figure 4: Main shape characteristics of typical office buildings

Reference buildings can be theoretical archetypes built on average data or real-reference buildings with characteristics similar to the median data [32]. In this study, a reference building was selected based on the characteristics mentioned above. As shown in Figure 5, the reference building has five floors with a building area of 6,630 m^2, a length of 78m, a width of 17m, and a height of 22.5m.

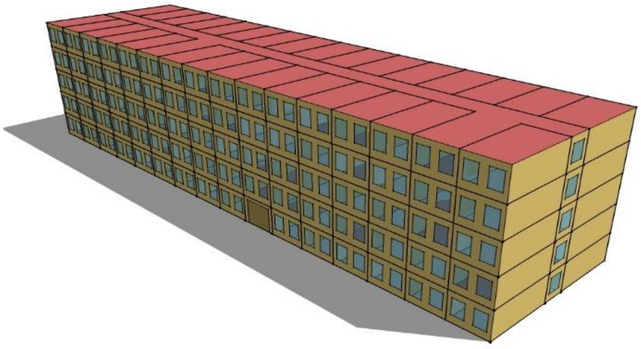

Figure 5: The simulation model of the reference building

.

2.4 Sensitivity analysis method

1) The Morris method

A building is a complex nonlinear system composed of many parameters with differing effects on building performance. Therefore, to reduce the complexity of the model, it is necessary to select the parameters that most critically affect the building performance analysis (BPA). As a powerful tool, sensitivity analysis (SA) has received increasing attention due to its outstanding performance in BPA. SA is mainly divided into local sensitivity analysis (LSA) and global sensitivity analysis (GSA). LSA is a one-factor-at-a-time method where the value of one parameter changes whilst the values of other parameters remain fixed. LSA has the advantage of simple and rapid computation. Compared with LSA, GSA can calculate the effect of the interaction between variables on the model output results and can provide more sensitivity information, but the calculation process is complicated.

GSA includes regression-based methods and screening-based, variance-based and meta-modelling approaches. Among them, the most widely used sensitivity analysis method is the screening-based Morris method which is computationally fast and suitable for models with a large number of parameters. To determine the accuracy of the Morris method, Kristensen *et al.* [33] compared the performance of Sobol and Morris in the building energy model, and the results showed that the Morris method leads to the same identification and ranking of parameters as the more accurate Sobol method when the variation of inputs is uniformly distributed between the boundaries. However, the Morris method is dozens of times faster than that of Sobol.

The Morris sensitivity method was proposed by Morris in 1991 [34], and it is widely used in the field of building performance because of its ease of operation, high accuracy, and low computational effort to identify the importance of the influence of different parameters on the output variables [35]. The method indicates the importance of each input parameter by calculating two sensitivity indicators μ_i and σ_i. μ_i represents the sensitivity intensity of the ith variable, when a larger μ_i indicates that the variable has a greater degree of influence on the output result, i.e., the parameter is more important. σ_i represents the fluctuation of the importance of the ith variable on a given interval, reflecting the interaction between the variables or the nonlinear relationship between the input and output variables. To avoid positive and negative offsets due to interactions between parameters, Campolong *et al.* [36] proposed a new indicator μ_i^*, which provides the absolute value of importance. μ_i^*, μ_i, and σ_i become the indicators of sensitivity analysis for the Morris sensitivity analysis method.

In sensitivity analysis, there are thousands of different combinations of different design parameters. It is obviously impossible to analyze the possible values of all parameters one by one. Therefore, each parameter needs to be sampled in its defined interval, and the sampling method determines the accuracy of the sensitivity analysis results. Morris *et al.* [34] proposed a sampling method based on trajectory. As shown in Figure 6, by changing a fixed step length for each parameter in the entire multi-dimensional parameter space, a sampling trajectory which contains the changes of all parameters is established, while taking into account the inner influence of multiple parameters. By randomly creating multiple trajectories in the parameter space, the sensitivity index for each parameter is calculated.

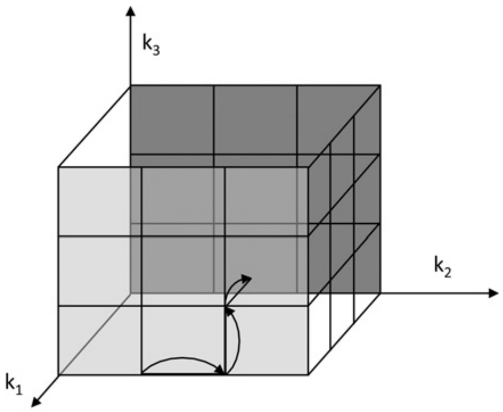

Figure 6: Morris sampling method [37]

Morris provided the calculation formula for a trajectory [37], based on the trajectory calculation matrix B* of a random matrix, as shown in formulae (3) and (4)

$$B^* = \left(J_{m,1}x^* + \Delta B'\right)P^* \qquad (3)$$

$$B^* = \left(J_{m,1}x^* + \left(\frac{\Delta}{2}\right)\left[\left(2B - J_{m,k}\right)D^* + J_{m,k}\right]\right)P^* \qquad (4)$$

Here, P^* is the permutation matrix, which is a randomly generated matrix. In each row and each column, there can only be one position of 1 and the remaining positions of 0. It is mainly used to exchange the positions of parameters and generate as many trajectories as possible. B' is a random position unique matrix, which determines whether the direction of the sampling trajectory changes in the positive or the negative direction, as shown in the calculation formula (5).

$$B' = 0.5\left[\left(2B - J_{m,k}\right)D^* + J_{m,k}\right] \qquad (5)$$

Where $J_{m,k}$ is a '1' matrix with m rows and k columns, k is the number of variables, m is equal to k plus 1, and B is a sampling unit matrix with m rows and k columns composed of only 0 and 1, D* is a k-dimensional diagonal matrix composed of 1 or (-1).

After the establishment process of the above-mentioned trajectory matrix, it is possible to calculate sample proof formed by different combinations of many parameters. By calculating the value of EE_i of each parameter on each trajectory on energy consumption, and integrating all the sampled trajectories, the corresponding parameters of each parameter can be calculated, see formulae (6-9).

$$EE_i = \frac{F\ (x_1,\cdots x_i+\Delta\cdots x_n)-F\ (x_1,\cdots x_i\cdots x_n)}{\Delta} \quad (6)$$

$$\mu_i = \frac{\sum_{i=1}^{r} EE_i}{r} \quad (7)$$

$$\sigma_i = \sqrt{\frac{1}{r}\sum_{i=1}^{r}(EE_i-\mu_i)^2} \quad (8)$$

$$\mu_i^* = \frac{\sum_{i=1}^{r}|EE_i|}{r} \quad (9)$$

where r represents the number of levels of x_i within its value range, Δ is the change of the parameter x_i relative to the reference value, and $F(x)$ represents the calculation equation or calculation model.

In this study, we mainly examine the impact of different design parameters on energy consumption. EnergyPlus simulation software is used to calculate energy consumption for heating and cooling, the Morris sampling method is used to extract different parameter combinations from the parameter value space, and the impact of different parameters from seven typical cities on building energy consumption is finally calculated.

2) Input setting of the Morris analysis model

The building is a complex system composed of a large number of parameters, many of which affect building energy consumption. Based on previous research results, passive design measures include improving thermal insulation, enhancing the airtightness, optimizing the window-to-wall ratio, and shading. The parameters involved in this study include thermal insulation performance (wall, roof), window performance (heat transfer coefficient /solar heat gain coefficient), airtightness, orientation, WWR (east, west, south, north), and shading (east, west, south, north).

The range of design parameters is shown in Table 5. The value of the building orientation is based on the 'Design standard for energy efficiency of public buildings' (GB50189-2015), and the value range is -30°C to 30°C. The value range of the external wall, roof, external window, window-to-wall ratio, and infiltration rate of the building is based on GB50189-2015 and GB/T51350-2019. The heat transfer coefficient of the roof and external walls can be changed by changing the thickness of the thermal insulation material XPS. The structure of the external walls and roofs are shown in Tables 6 and 7. The shading coefficient (SC) of the external shading is used as the design parameter for shading. In this paper, the Venetian blinds are only used when the direct sun intensity is greater than 100W/ m^2. According to the calculation method provided by the literature [38], when the Venetian blinds completely cover the outer windows, the shading coefficient is 0.4, and when the Venetian blinds are not used, the shading coefficient is 1.0. According to GB50189-2015, shading for the north is not required in the HSCW zone. Therefore, in this study, only three directions of shading (south, east, and west) are considered.

Since the study focuses on the application of passive design measures, similar to many previous studies [18, 25, 27, 39, 40], an Ideal Loads Air System is built in EnergyPlus. The "Ideal Loads Air System" is an ideal heating and cooling system to calculate the energy that must be added to or extracted from a space to maintain thermal comfort without specified the HVAC forms. The system can be assumed as an ideal unit that mixes air at the zone exhaust condition with the specified amount of outdoor air and then adds or removes heat and moisture to produce a supply air stream at the specified conditions [41]. The indoor thermal condition can be controlled within the design range by the 'Ideal Loads Air System'. Hundreds of passive design solutions are compared and analyzed in the same scenario of creating the same indoor thermal condition. According to GB 50189-2015, the occupancy schedule is 7:00~18:00, the cooling setpoint is 26℃ and the heating setpoint is 20℃. The power density of lighting and electrical equipment is 9.0 W/m^2 and 15 W/m^2, respectively. Electricity is the largest fuel for HVAC systems in office buildings in the Hot Summer and Cold Winter zone [30, 42]. To evaluate the electricity consumption of the most common HVAC devices (such as air-to-air heat pump) in office buildings, the heating and cooling demand calculated from the 'Ideal Load Air System' is converted into electricity usage. The Coefficient of Performance (COP) for heating is 2.5. The Energy Efficiency Ratio (EER) for cooling is 3.0. The shading coefficient of the external shading device ($SC_{shading}$) is defined as the ratio of the solar heat gain with shading measures to that without shading measures [43]. It can be calculated by equation (10) [29].

$$SC_{shading} = I_s/I_o \qquad (10)$$

Where I_s refers to the solar irradiation falling on the shaded fenestration (W), and I_o refers to the solar irradiation falling on the no fenestration if it is not shaded (W).

For the heat balance calculation, the Conduction Transfer Function algorithm provided by Energyplus is used and the number of timesteps per hour is 6. The weather file was downloaded from the EnergyPlus official weather website.

Table 5: The range of design parameters for the Morris method

Parameters	Description	Base value	Probability	Range
Orientation	Degrees from true North [°]	0	Continuous Uniform	[-30, 30]
U-value of exterior wall	[W/ m^2.K]	0.83	Discrete	(0.83,0.65,0.53,0.45,0.39, 0.35,0.31,0.28,0.26,0.24)
U-value of roof	[W/ m^2.K]	0.58	Discrete	(0.58,0.48,0.42,0.37, 0.33,0.30,0.27,0.24)
U-value of exterior window	[W/ m^2.K]	2.8	Discrete	（1.37,1.4,1.8,2.2,2.6）
SHGC of exterior window	SHGC	0.75	Discrete	(0.31,0.37,0.57,0.63,0.75)
Infiltration rate	[h^{-1}]	1.0	Discrete	（0.5,0.6,0.8,1.0）
Window-to-wall ratio	WWR_S	0.4	Continuous Uniform	[0.2, 0.70]
	WWR_N	0.4	Continuous Uniform	[0.2, 0.70]
	WWR_E	0.2	Continuous Uniform	[0.2, 0.70]
	WWR_W	0.2	Continuous Uniform	[0.2, 0.70]
Shading Coefficient of venetian blinds	$SC_{shading}$_S	1.0	Discrete	(0.4,1.0)
	$SC_{shading}$_E	1.0	Discrete	(0.4,1.0)
	$SC_{shading}$_W	1.0	Discrete	(0.4,1.0)

Table 6: The structure of the roof

NO.	Crushed Stone concrete （mm）	Cement mortar (mm)	XPS (mm)	SBS modified bitumen waterproofing membrane （mm）	Cement mortar (mm)	All-lightweight concrete (mm)	Reinforced Concrete (mm)	U-Value （W/ m^2.K）
1	20	20	40	5	20	30	20	0.58
2	20	20	50	5	20	30	20	0.48
3	20	20	60	5	20	30	20	0.42
4	20	20	70	5	20	30	20	0.37
5	20	20	80	5	20	30	20	0.33
6	20	20	90	5	20	30	20	0.29
7	20	20	100	5	20	30	20	0.27
8	20	20	120	5	20	30	20	0.24

Table 7: The structure of the wall

NO.	Cement mortar (mm)	XPS (mm)	Cement mortar (mm)	Sintered shale porous brick (mm)	Cement mortar (mm)	U-Value （W/ m^2.K）
1	5	20	20	200	20	0.83
2	5	30	20	200	20	0.65
3	5	40	20	200	20	0.53
4	5	50	20	200	20	0.45
5	5	60	20	200	20	0.39
6	5	70	20	200	20	0.35
7	5	80	20	200	20	0.31
8	5	90	20	200	20	0.28
9	5	100	20	200	20	0.26
10	5	120	20	200	20	0.24

2.5 Multi-objective optimization method

In the multi-objective optimization model, the input variables are parameters that have an essential influence on $EUI_{H\&C}$ screened out through Morris, and the other parameters keep their reference values. Python is used to embed EnergyPlus into NSGA-II to input parameters to the model, read the results, and control the optimization process. The main optimization process of this research is as follows, and is shown in Figure 7:

1) Set input parameters: as shown in Table 5, there are 13 input parameters, including the external wall heat transfer coefficient, roof heat transfer coefficient, heat transfer coefficient, solar heat gain coefficient of glass, airtightness, and shading.
2) NSGA-II parameter setting: the parameters of the algorithm include population size, mutation rate, evolution times, and the number of parallel computing processes. In this study, the population size is 100, the mutation rate is 0.4, the evolution number is 100, and the number of parallel computing processes is 96.
3) Optimization process: first, the initial population is randomly generated according to the NSGA algorithm; second, in the initial population, the values of the objective functions of each individual are calculated by EnergyPlus; third, the non-dominated sorting of each individual is applied based on the values of the objective functions; fourth, the crowded distance is calculated between each individual and their neighbors; fifth, according to the calculation results of the third and fourth steps, the outstanding individuals of the initial population are selected as the next generation population. Repeat the cycle from the first to the fifth step until the maximum number of evolutions is reached. Through continuous evolution, outstanding individuals are gradually preserved to form the Pareto solutions set.

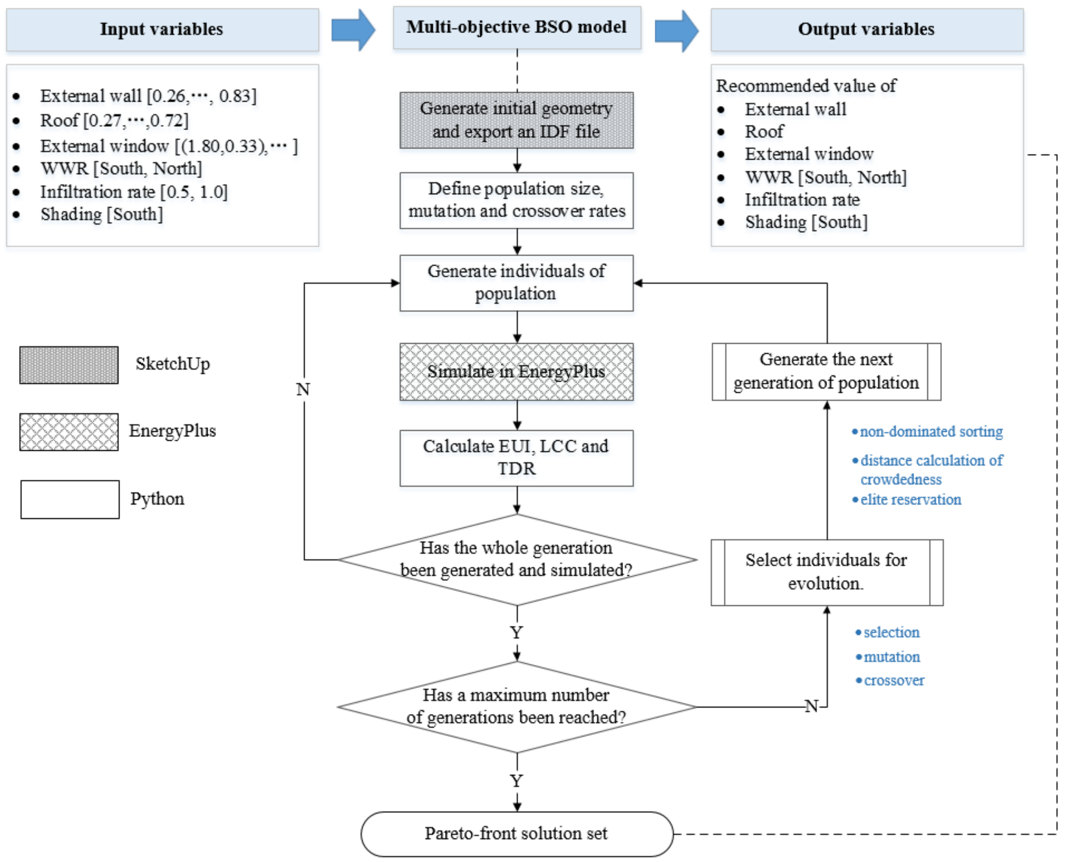

Figure 7: The flow chart of NSGA-II[44]

As described above, the objectives of this study are the energy consumption intensity of HVAC ($EUI_{H\&C}$), the percentage of uncomfortable hours in transition seasons (PUH), and the life cycle cost (LCC). The constraint equation of the objective function can be described as (11):

$$\begin{cases} Minimize\ F_1\ (x) = EUI_{H\&C} \\ Minimize\ F_2\ (x) = PUH \\ Minimize\ F_3\ (x) = LCC \end{cases} \tag{11}$$

Energy consumption intensity of HVAC ($EUI_{H\&C}$)

Based on background research, in this study, the energy consumption of the annual heating and cooling is calculated by EnergyPlus. The $EUI_{H\&C}$ can be expressed by the annual electricity consumption per unit air-conditioning area in $kW \cdot \frac{h_e}{m^2_{AC}}$. The energy consumption calculation formula is (12):

$$EUI_{H\&C} = \frac{1}{A_{AC}} \times (E_H + E_C) \tag{12}$$

Note: A_{AC} is the air-conditioning area in m^2, E_H is the annual electricity consumption of heating in kWh, and E_C is the annual electricity consumption of cooling in kWh.

Percentage of uncomfortable hours in transition seasons (PUH)

In the heating and cooling seasons, a comfortable indoor thermal environment is created using heating and cooling equipment. When the equipment is active, the indoor environment can remain relatively stable and comfortable. However, in transition seasons, creating the indoor thermal environment mainly relies on passive methods, such as natural ventilation and shading, which are extremely susceptible to the influence of the outdoor environment, resulting in over-cooling or over-heating. To maintain a comfortable thermal environment during transition seasons, while extending the non-heating and air-conditioning time, the percentage of discomfort hours in transition seasons is used as the objective function; the calculation is shown in (13):

$$\mathrm{PUH} = \frac{DH}{N} \times 100\% \tag{13}$$

Note: N is the occupied hours during the transition seasons, and DH is the discomfort hours during the transition seasons.

A transition season is the non-artificial thermal environment and is not suitable for directly adopting the PMV-PPD model proposed by Fanger. As an effective evaluation method, aPMV is widely used in the evaluation of indoor thermal comfort levels in non-artificial thermal environments. In the "Evaluation standard for the indoor thermal environment in civil buildings" (GB/T 50785-2012), the indoor thermal comfort level of the non-artificial thermal environment is classified as shown in Table 8. In this study, the number of hours that aPMV is beyond the range of level I (-0.5≤aPMV≤0.5) was defined as the uncomfortable hours. The number of uncomfortable hours in transition seasons is counted and represented as a percentage. The smaller the PUH, the higher the indoor comfort.

Table 8: Thermal comfort level in the non-artificial cold and heat source intervention environment

Level	Assessment Criteria (aPMV)
I	－0.5≤APMV≤0.5
II	－1≤aPMV＜－0.5 or 0.5＜aPMV≤1
III	aPMV＜－1 or aPMV＞1

According to the aPMV calculation method provided by Yao *et al.* [45], the calculation relationship between the aPMV and PMV models is established, as shown in equation (14).

$$aPMV = \frac{PMV}{1+\lambda PMV} \tag{14}$$

According to GB/T 50785-2012, in the HSCW zone, when PMV≥0, λ is 0.21 and when PMV <0, λ is -0.49. The thermal comfort module in EnergyPlus provides the classic Fanger model to calculate the hourly PMV throughout the year.

Life cycle cost

The building design solutions must not only achieve the goals of energy-saving and comfort but also be economically feasible. The economic evaluation method of life cycle cost (LCC) is usually adopted for construction projects. LCC is divided into two categories according to whether the static or dynamic method is used to consider the time value of costs.

Due to the long service life of buildings, it is necessary to consider the impact on costs of bank interest rates, inflation and discount rate fluctuations, and the time value of costs. This study uses the dynamic method where the initial investment and operating costs related to $EUI_{H\&C}$ are considered. The LCC analysis method based on net present value is adopted, and the cost analysis period is set at 20 years. The equation for LCC can be expressed by equation (15) to (20).

$$\mathrm{LCC} = C_{in} + C_o \tag{15}$$

where LCC is the net present value of the analysis period, CNY/ m^2; C_{in} is the net present value of the initial investment of the energy efficiency measures, CNY/ m^2; and C_o is the net present value of the energy costs for heating and cooling in the analysis period, CNY/ m^2.

$$C_{in} = \frac{C_{\mathrm{wall}} + C_{\mathrm{win}} + C_{\mathrm{roof}} + C_{\mathrm{shd}} + C_{\mathrm{inf}}}{A_{AC}} \tag{16}$$

$$C_{\mathrm{wall}} = \left(C_{i-\mathrm{wall}} \cdot \delta_{\mathrm{wall}} + C_{e-wall}\right) \cdot A_{wall} \tag{17}$$

$$C_{\mathrm{roof}} = \left(C_{i-roof} \cdot \delta_{\mathrm{roof}} + C_{e-roof}\right) \cdot A_{roof} \tag{18}$$

$$C_{win} = \left(C_{i-win} + C_{e-win} + C_{infil} + C_{shd}\right) \cdot A_{win} \tag{19}$$

$$C_o = EUI_{H\&C} \cdot C_e[1 - (1 + I)^{-N}]/I \tag{20}$$

where $\mathrm{C_{i-wall}}$ and $\mathrm{C_{i-roof}}$ are the price of thermal insulation materials per unit volume of exterior walls and roof, CNY/ m^3; δ_{wall} and δ_{roof} are the thickness of thermal insulation material of the exterior walls and roof, m; $\mathrm{C_{i-win}}$ is the price per unit area of glass, CNY/ m^2; $\mathrm{C_{e-wall}}$, $\mathrm{C_{e-win}}$ and $\mathrm{C_{e-roof}}$ are the respective installation labor costs of insulation materials per unit area of external walls, external windows, and roofs**,** CNY/ m^2; $\mathrm{C_{inf}}$ is the increased cost for improving the airtightness of the building, CNY/ m^2; $\mathrm{C_{shd}}$ is the cost of shading facilities, CNY/ m^2; $\mathrm{A_{wall}}$, $\mathrm{A_{win}}$ and $\mathrm{A_{roof}}$ are the area of the exterior walls, exterior windows, and roof, respectively; A_{AC} is the total air-conditioned area, m^2; $EUI_{H\&C}$ is the annual energy consumption intensity of heating and cooling per unit air-conditioned area, kWh/ m^2; C_e is the local electricity price, CNY/ kWh; N is the analysis period in years; I is the bank interest rate, %. The average price of office electricity in the HSCW zone of the State Grid in 2018 was 1.2 CNY/ kWh; the analysis period is 20 years, and the bank loan interest rate is 4.9% based on the Bank of China interest rate (accessed date: June 15,2018). Information on the costs of construction materials was obtained from an investigation of manufacturers in different cities. The price of the insulation material XPS is 712.77 CNY/m^3. The price of ordinary insulating glass is 116.51 CNY /m^2, the price of triple glazing is 266 CNY/ m^2, the price of LOW-E insulating glass is 163.39 CNY /m^2, and the installation labor cost is 30 CNY/ m^2.

The input interface of the multi-objective model is shown in Figure 8.

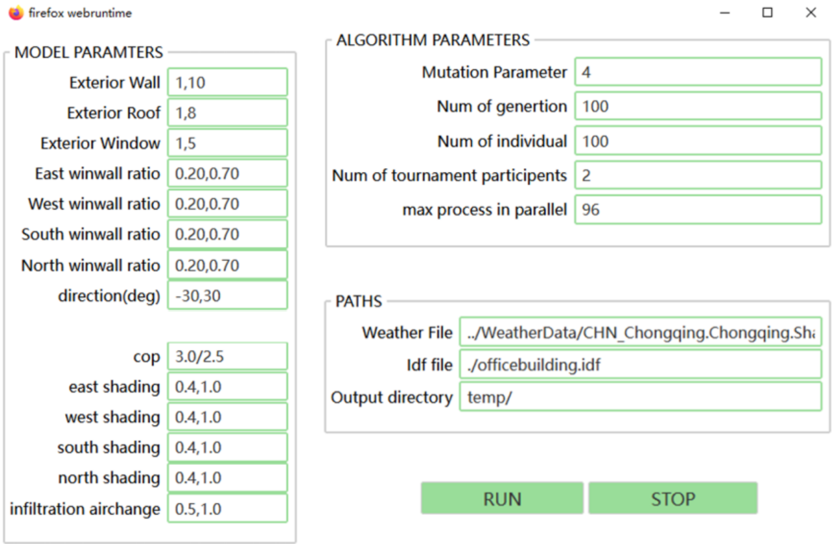

Figure 8: The input interface of the multi-objective model

2.6 The multi-criteria decision-making method

Multi-criteria decision-making methods can help decision-makers choose the best solution from the Pareto solution set obtained by the multi-objective optimization model. Compared with other decision-making methods, TOPSIS is more efficient and faster when dealing with a large number of solutions and attributes. TOPSIS has been successfully applied for building performance evaluation in several studies [44] [46] [47]. TOPSIS is based on calculating the Euclidean distance of an alternative solution from the ideal solution. An alternative solution will be selected when it has the shortest Euclidean distance from the positive ideal point and the farthest Euclidean distance from the negative ideal point. The ranking of alternatives is based on the comparison of these Euclidean distances.

As shown in Figure 9, the green point represents the positive ideal solution, the blue point represents the negative ideal solution, and the red points represent all alternative solutions in the Pareto solution set. The solution closest to the green point is the optimal solution, which is denoted by the red star. A more detailed calculation process can be found in [46].

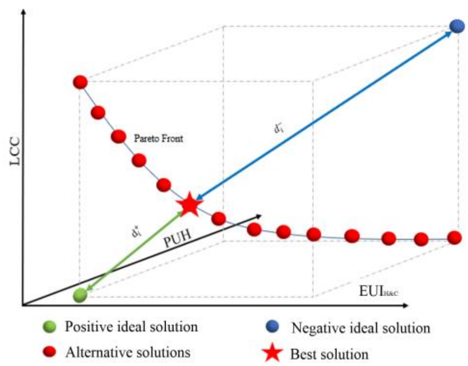

Figure 9: Schematic diagram of TOPSIS

3 Results

3.1 Sensitivity study

In this paper, the Morris diagram is used to present the sensitivity analysis results of different design parameters of each climate sub-zone, as shown in Figure 10. The X-axis of the Morris chart represents the average value μ_i, and the Y-axis represents the mean square error σ_i. When the X-axis value is very small, the parameter has little influence on the output result; when the X-axis value is large, the parameter has a strong non-linear relationship with the output. When the value of the Y-axis is small, the correlation between this parameter and other parameters is weak. However, when the values of the X-axis and Y-axis are both large, the parameter has a strong impact on the model output, and the correlation between this parameter and other parameters is strong.

Figure 10 shows the Morris diagram of the sensitivity analysis results of the A2 climate sub-zone. The A2 climate sub-zone is an area with medium heating demand and high cooling demand. As shown in Figure 10, the infiltration rate is the most significant factor affecting heating and cooling demand and has a high correlation with other design parameters. The SHGC of the window has a greater impact on the cooling demand, less on the heating demand, and a lower correlation with other design parameters. The south and north window-to-wall ratios, the heat transfer coefficient of the exterior window, and the heat transfer coefficient of the exterior wall have a greater influence on the heating demand in winter. From the perspective of total heating and cooling demand, the infiltration rate, SHGC of the window, the south window-to-wall ratio and south shading should be considered in the design solution for the A2 climate sub-zone.

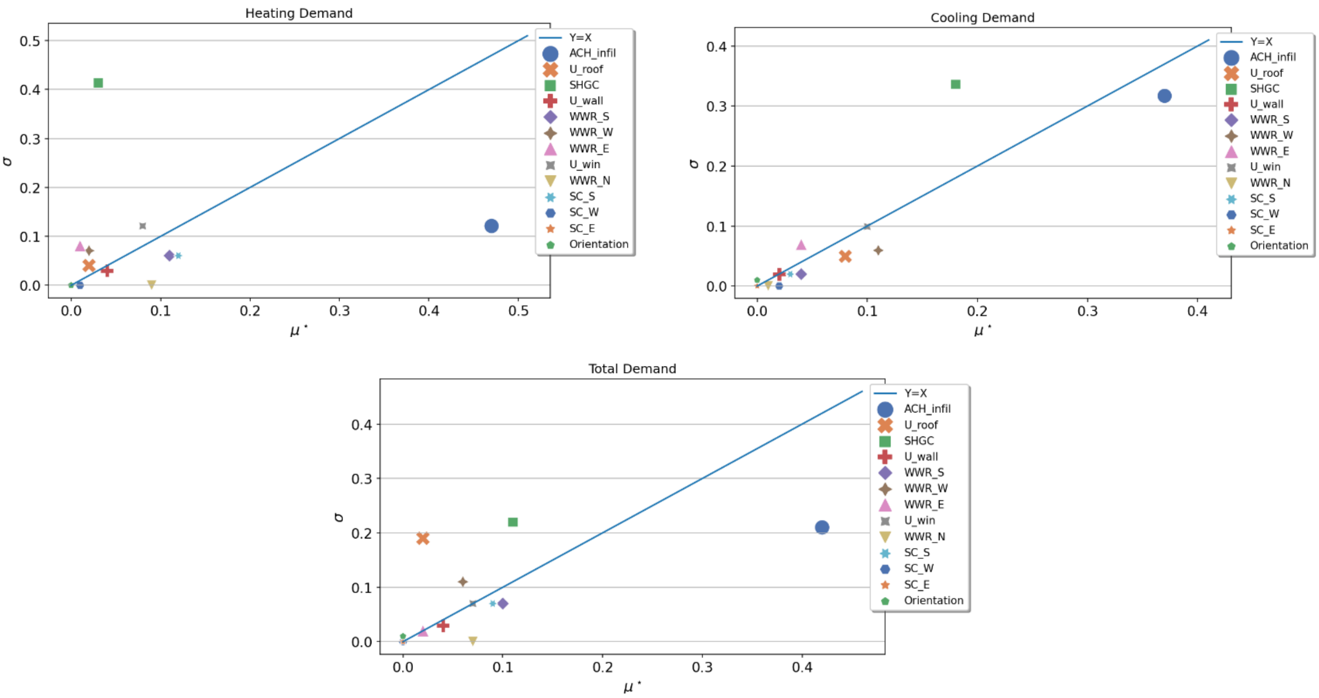

Figure 10: Sensitivity analysis of design parameters to total heating and cooling energy demand for the A2 climate sub-zone

Figure 11 shows the ranking of sensitivity indicators for different design factors of heating energy demand, cooling energy demand, and total heating and cooling energy demand in different climate sub-zones. For total heating and cooling energy demand, the top 10 design factors of sensitivity index are ACH_Infil, U_roof, SHGC, U_wall, WWR_S, WWR_W, WWR_E, U_win, WWR_N, SC_S. The top 10 parameters are set as variables in the optimization model, and the remaining design parameters are set as fixed values.

	Heating demand							Cooling demand							Total heating & cooling demand						
Sub-climate zone	A1	A2	A3	B1	B2	C1	C2	A1	A2	A3	B1	B2	C1	C2	A1	A2	A3	B1	B2	C1	C2
ACH_infil	1	1	1	1	1	1	1	1	1	1	1	1	1	1	1	1	1	1	1	1	1
U_roof	3	7	5	2	8	5	8	7	2	3	8	2	2	2	2	2	2	2	2	2	2
SHGC	6	3	10	4	3	3	2	2	6	2	7	7	6	6	3	3	3	3	3	3	3
U_wall	2	2	11	3	2	2	3	9	8	4	4	8	8	8	4	4	4	4	4	4	4
WWR_S	4	5	4	7	4	4	4	4	4	5	2	4	4	4	5	5	5	5	5	5	5
WWR_W	8	4	6	9	9	9	10	3	11	6	3	3	3	3	6	6	6	6	6	6	6
WWR_E	5	8	2	6	7	7	6	11	3	8	10	5	11	5	7	7	7	7	7	7	7
U_win	11	6	3	5	5	8	5	6	10	9	11	10	5	10	8	8	8	8	8	8	8
WWR_N	10	9	8	8	11	11	11	5	5	7	5	6	7	7	9	9	9	9	9	9	9
SC_S	7	11	12	11	6	6	7	10	7	10	6	11	10	11	10	10	10	10	10	10	10
SC_W	9	10	9	12	10	10	9	8	9	11	12	9	9	9	11	11	11	11	11	11	11
SC_E	12	12	7	10	12	12	12	12	12	12	9	12	12	12	12	12	12	12	12	12	12
Orientation	13	13	13	13	13	13	13	13	13	13	13	13	13	13	13	13	13	13	13	13	13

The most significant factor Ranking The least significant factor

1	2	3	4	5	6	7	8	9	10	11	12	13

Figure 11: Sensitivity ranks of different parameters for different climate sub-zones

3.2 Optimization

The multi-objective optimization result of NSGA-II is a Pareto non-dominated solution set, which contains all alternative solutions. The objective function of each solution in the solution set is drawn into a three-dimensional scatter plot（Figure 12), and the three-dimensional plot is projected onto each coordinate plane for analysis, as shown in Figure 13. The grey points in Figure 12 represent the initial population randomly generated by NSGA-II, and the distribution is very scattered. After 100 generations of iterative optimization, a non-dominated Pareto solution set that weighs three objectives is obtained, which is represented by red points. In the Pareto solution concentration, $EUI_{H\&C}$ of different solutions varies from 31.5 kWh/ m^2~39.3 kWh/ m^2, DHR varies from 0.59 to 0.76, and LCC varies from 1980 to 6300 CNY/ m^2. As shown in Figure 14, there is a mutual restriction relationship between LCC and $EUI_{H\&C}$, a mutual restriction relationship between LCC and PUH, and there is a positive correlation between $EUI_{H\&C}$ and PUH. A decrease in $EUI_{H\&C}$ will cause an increase in LCC and a decrease in PUH. With the continuous improvement in building envelope performance, $EUI_{H\&C}$ decreases, and LCC increases at different rates; $EUI_{H\&C}$ was reduced from 39.3 kWh/ m^2 to 32.6 kWh/ m^2, LCC increased from 1980 to 2395 CNY/ m^2, the number of thermal discomfort hours in the transitional season was reduced from 0.76 to 0.63, $EUI_{H\&C}$ was reduced by 17%, PUH decreased by 21%, and LCC increased by 20%. However, when energy consumption is reduced from 32.6 kWh/ m^2 to 31.5 kWh/ m^2, $EUI_{H\&C}$ is reduced by 3%, PUH is reduced by 6%, and LCC is increased by 60%. Therefore, in the energy-saving optimization design of buildings, it is necessary to consider the costs of the solutions; the costs of the proposed building design solution must be within an acceptable range to the property developers, so they are feasible and easier to promote on a large scale.

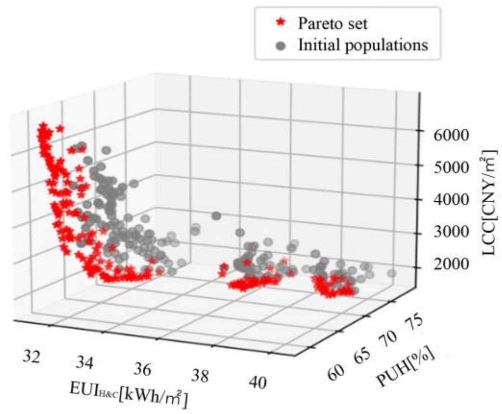

Figure 12: The Pareto set of multi-objective optimization (A2)

Through the analysis of the Pareto solution set of seven typical cities, it can be seen that the ranges of $EUI_{H\&C}$, DHR and LCC are different for each typical city due to different climatic factors. However, the mutual constraints between the three objectives are all consistent. It is necessary to consider $EUI_{H\&C}$, LCC, and DHR, and determine the optimal plan from the Pareto solution set.

3.3 Decision-making

In this section, we apply the TOPSIS decision-making method to rank all the solutions in the Pareto solution set, select the first-ranked solution as the best solution, and choose the top 20 solutions as the recommended solutions for each climate sub-zone (Figure 13).

We take the A2 climate sub-zone as an example to analyze the TOPSIS decision results in detail. Table 9 shows the calculation results of the top 20 solutions for the A2 climate sub-zone, including decision matrix D, normalize matrix R, weighted matrix V, and Euclidean distance. It can be seen from Table 9 that the $EUI_{H\&C}$ of the best solution is 32.93 kWh/ m^2, the PUH is 63.71%, and the LCC is 2290.67 CNY /m^2. Among the top 20 solutions, $EUI_{H\&C}$ varies from 32.77 kWh/m^2 to 33.38 kWh/m^2, PUH varies from 62.1% to 66.13%, and LCC varies from 2180.64 CNY /m^2 to 2411.33 CNY /m^2. The distribution of the top 20 solutions in the Pareto solution set is shown by the red dots in Figure 13.

Table 10 shows the design parameters of the top 20 solutions. U_wall varies from 0.53 to 0.83, U_roof varies from 0.48 to 0.58, U_win varies from 1.37 to 2.6, SHGC varies from 0.31 to 0.75, and WWR varies from 0.2 to 0.7. All the top 20 solutions recommend an infiltration rate of 0.5 and south shading.

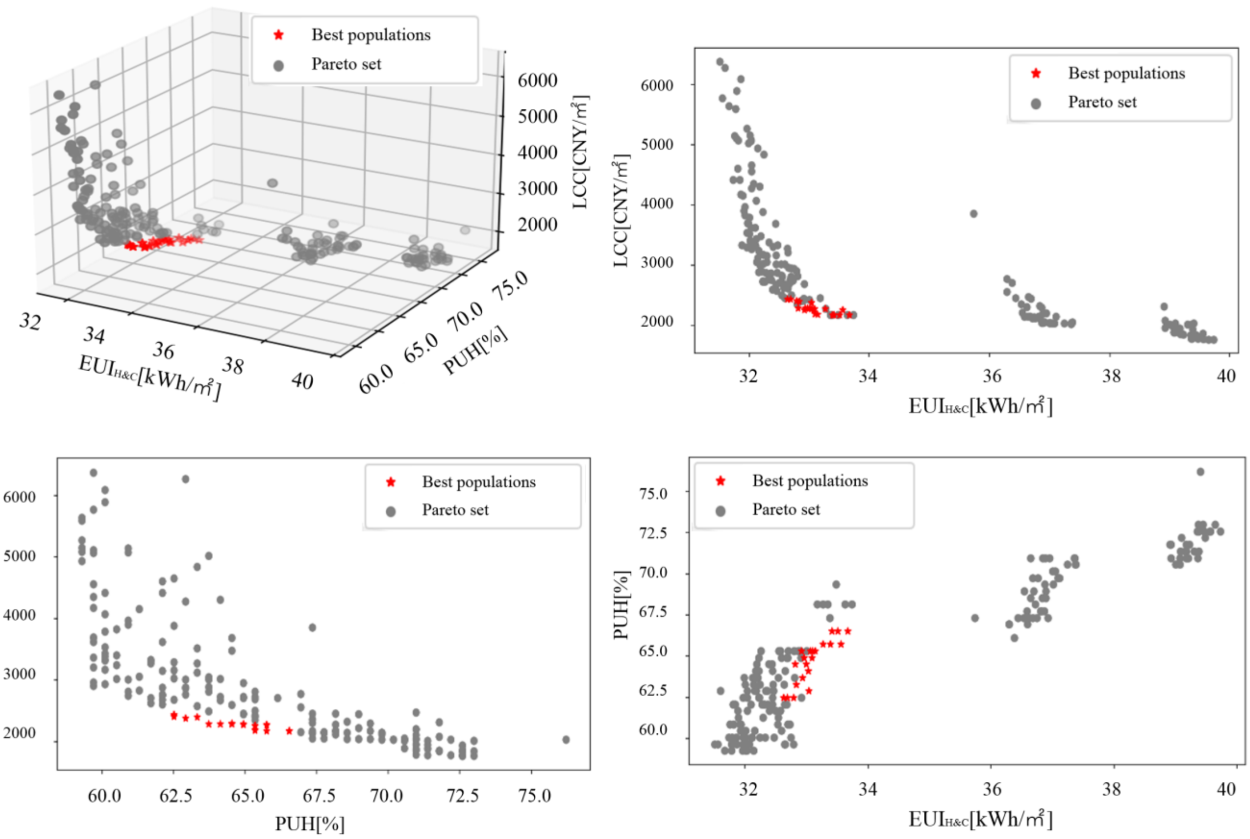

Figure 13: Distribution of TOPSIS decision results in Pareto for the A2 climate sub-zone

Table 9: The result of the TOPSIS in Changsha

Decision matrix D			Normalize matrix R			Weighted matrix V			Euclidean distance			Rank
$EUI_{H\&C}$	PUH	LCC	$EUI_{H\&C}$	PUH	LCC	$EUI_{H\&C}$	PUH	LCC	D^+	D^-	C^*	
32.93	63.71	2290.67	0.0540	0.1045	0.0395	0.0178	0.0345	0.0130	0.0242	0.0039	0.1383	1
33.03	64.11	2285.46	0.0542	0.1051	0.0394	0.0179	0.0347	0.0130	0.0242	0.0040	0.1424	2
32.90	62.10	2400.67	0.0540	0.1018	0.0414	0.0178	0.0336	0.0137	0.0239	0.0040	0.1427	3
33.23	65.32	2188.12	0.0545	0.1071	0.0377	0.0180	0.0354	0.0125	0.0246	0.0042	0.1445	4
33.03	62.90	2383.14	0.0542	0.1032	0.0411	0.0179	0.0340	0.0136	0.0238	0.0041	0.1464	5
33.00	64.52	2284.94	0.0541	0.1058	0.0394	0.0179	0.0349	0.0130	0.0242	0.0042	0.1469	6
32.79	62.50	2411.33	0.0538	0.1025	0.0416	0.0177	0.0338	0.0137	0.0238	0.0041	0.1473	7
33.32	65.73	2181.24	0.0547	0.1078	0.0376	0.0180	0.0356	0.0124	0.0246	0.0043	0.1495	8
33.38	65.73	2180.90	0.0547	0.1078	0.0376	0.0181	0.0356	0.0124	0.0246	0.0043	0.1497	9
33.04	65.73	2192.80	0.0542	0.1078	0.0378	0.0179	0.0356	0.0125	0.0245	0.0043	0.1498	10
32.96	64.52	2309.38	0.0540	0.1058	0.0398	0.0178	0.0349	0.0131	0.0240	0.0043	0.1504	11
33.09	64.92	2282.65	0.0543	0.1065	0.0394	0.0179	0.0351	0.0130	0.0241	0.0043	0.1516	12
32.84	64.92	2295.06	0.0539	0.1065	0.0396	0.0178	0.0351	0.0131	0.0241	0.0043	0.1526	13
32.96	65.32	2258.12	0.0541	0.1071	0.0390	0.0178	0.0354	0.0129	0.0242	0.0044	0.1527	14
33.01	65.32	2259.92	0.0541	0.1071	0.0390	0.0179	0.0354	0.0129	0.0242	0.0044	0.1531	15
32.83	63.31	2406.74	0.0538	0.1038	0.0415	0.0178	0.0343	0.0137	0.0237	0.0043	0.1535	16
32.95	65.32	2265.59	0.0540	0.1071	0.0391	0.0178	0.0354	0.0129	0.0242	0.0044	0.1537	17
33.27	66.13	2180.64	0.0546	0.1084	0.0376	0.0180	0.0358	0.0124	0.0245	0.0045	0.1546	18
32.77	64.52	2356.75	0.0537	0.1058	0.0407	0.0177	0.0349	0.0134	0.0238	0.0044	0.1572	19
32.93	63.71	2290.67	0.0540	0.1045	0.0395	0.0178	0.0345	0.0130	0.0242	0.0039	0.1383	20

Table 10: Recommended design plan and parameter value range of A2

Rank	$EUI_{H\&C}$	PUH	LCC	U_wall	U_roof	U_win	SHGC	WWR_E	WWR_W	WWR_S	WWR_N	SC_S	ACH_Infil
1	32.93	63.71	2290.67	0.65	0.58	1.37	0.31	0.41	0.20	0.26	0.48	0.4	0.5
2	33.03	64.11	2285.46	0.83	0.58	1.40	0.37	0.25	0.25	0.20	0.29	0.4	0.5
3	32.90	62.10	2400.67	0.65	0.58	1.37	0.31	0.57	0.22	0.40	0.49	0.4	0.5
4	33.23	65.32	2188.12	0.83	0.58	1.37	0.31	0.34	0.29	0.27	0.30	0.4	0.5
5	33.03	62.90	2383.14	0.65	0.58	1.37	0.31	0.48	0.23	0.20	0.57	0.4	0.5
6	33.00	64.52	2284.94	0.83	0.58	2.20	0.63	0.21	0.20	0.34	0.36	0.4	0.5
7	32.79	62.50	2411.33	0.65	0.58	1.37	0.31	0.35	0.24	0.34	0.20	0.4	0.5
8	33.32	65.73	2181.24	0.53	0.58	1.37	0.31	0.70	0.26	0.70	0.43	0.4	0.5
9	33.38	65.73	2180.90	0.53	0.58	1.37	0.31	0.28	0.23	0.54	0.43	0.4	0.5
10	33.04	65.73	2192.80	0.65	0.58	1.37	0.31	0.48	0.35	0.39	0.59	0.4	0.5
11	32.96	64.52	2309.38	0.65	0.58	1.37	0.31	0.31	0.28	0.36	0.51	0.4	0.5
12	33.09	64.92	2282.65	0.83	0.48	1.37	0.31	0.29	0.37	0.26	0.30	0.4	0.5
13	32.84	64.92	2295.06	0.83	0.48	1.40	0.37	0.35	0.25	0.20	0.42	0.4	0.5
14	32.96	65.32	2258.12	0.53	0.58	1.37	0.31	0.34	0.22	0.30	0.30	0.4	0.5
15	33.01	65.32	2259.92	0.53	0.58	1.37	0.31	0.32	0.20	0.34	0.20	0.4	0.5
16	32.83	63.31	2406.74	0.53	0.58	1.37	0.31	0.40	0.24	0.55	0.42	0.4	0.5
17	32.95	65.32	2265.59	0.83	0.58	2.20	0.63	0.22	0.24	0.31	0.37	0.4	0.5
18	33.27	66.13	2180.64	0.83	0.58	2.60	0.75	0.37	0.22	0.24	0.28	0.4	0.5
19	32.77	64.52	2356.75	0.83	0.58	2.60	0.75	0.32	0.20	0.40	0.43	0.4	0.5
20	32.93	63.71	2290.67	0.65	0.58	2.60	0.75	0.31	0.20	0.45	0.51	0.4	0.5
Recommended value range			min	0.53	0.48	1.37	0.31	0.21	0.20	0.20	0.20	0.4	0.5
			max	0.83	0.58	2.60	0.75	0.70	0.37	0.70	0.59	0.4	0.5

Table 11 shows the best solution and recommended solutions for the 7 climate sub-zones. For the best solutions in all climate sub-zones, U_wall varies from 0.65 to 0.83, U_roof varies from 0.37 to 0.58, U_win varies from 1.37 to 2.2, SHGC varies from 0.31 to 0.63, and WWR varies from 0.20 to 0.45. The infiltration rate in all climate sub-zones is 0.5 h^{-1}.

It should be emphasized that safety should be taken into account when installing and applying the venetian blinds. For the reference building in this study, which is a small and medium-sized office building, well-installed venetian blinds are recommended (Figure 14a and Figure 14b). However, for the high-rise office buildings or super high-rise office buildings, built-in venetian blinds windows or other energy-efficient products can be applied instead (Figure 14c)."

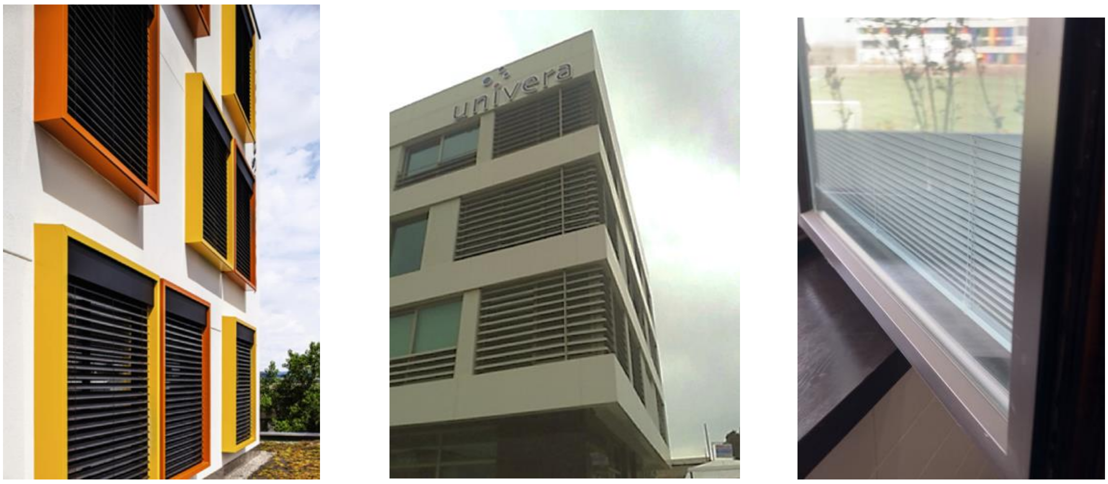

a) Curved blinds in roller shade [48]; b) Horizontal louvers [49]; c) a window with built-in venetian blinds (picture: the author)

Figure 14 Examples of venetian blinds

For the A1 climate sub-zone, compared to the base solution, the best solution, which ranked first among the options, consumed 19.5% less energy, reduced occupants' discomfort time by 6.1%, but increased costs by 361.47 CNY/ m^2. For the A2 climate sub-zone, compared to the base solution, the best solution, which ranked first among the options, consumed 16.1% less energy, reduced occupants' discomfort time by 11.2%, but increased costs by 326.95 CNY/m^2. For the A3 climate sub-zone, compared to the base solution, the best solution, which ranked first among the options, consumed 15.4% less energy, reduced occupants' discomfort time by 17.7%, but increased costs by 361.76 CNY/ m^2. For the B1 climate sub-zone, compared to the base solution, the best solution, which ranked first among the options, consumed 21.1% less energy, reduced occupants' discomfort time by 21.6%, but increased costs by 423.36 CNY/ m^2. For the B2 climate sub-zone, compared to the base solution, the best solution, which ranked first among the options, consumed 18.8% less energy, reduced occupants' discomfort time by 10.3%, but increased costs by 350.53 CNY/m^2. For the C1 climate sub-zone, compared to the base solution, the best solution, which ranked first among the options, consumed 20.7% less energy, reduced occupants' discomfort time by 10.4%, but increased costs by 444.62 CNY/m^2. For the C2 climate sub-zone, compared to the base solution, the best solution, which ranked first among the options, consumed 19.0% less energy, reduced occupants' discomfort time by 20.8%, and increased costs by 430.06 CNY/m^2. Illustrated as an average for each city, compared to the base solution, the best solutions in each city consume 18.7% less energy, reduce occupant discomfort time by 14.0%, but increase costs by 385.54 CNY/m^2.

Table 11: Energy-saving design solutions for office buildings in the HSCW zone

Climate Zone	Description		$EUI_{H\&C}$	PUH	LCC	U_wall	U_roof	U_win	SHGC	WWR_E	WWR_W	WWR_S	WWR_N	SC_S	ACH_Infil
A1	*Best solution*		*31.24*	*75.00*	*2166.69*	*0.83*	*0.58*	*1.37*	*0.31*	*0.39*	*0.27*	*0.37*	*0.24*	*Venetian blinds*	*0.5*
	Recommended value range	Min	30.81	74.19	2147.75	0.65	0.48	1.37	0.31	0.20	0.20	0.30	0.20	Venetian blinds	0.5
		Max	31.96	77.02	2384.12	0.83	0.58	2.60	0.75	0.47	0.37	0.56	0.51	Venetian blinds	0.5
A2	*Best solution*		*32.93*	*63.71*	*2290.67*	*0.65*	*0.58*	*1.37*	*0.31*	*0.41*	*0.20*	*0.26*	*0.48*	*Venetian blinds*	*0.5*
	Recommended value range	Min	32.77	62.10	2180.64	0.53	0.48	1.37	0.31	0.21	0.20	0.20	0.20	Venetian blinds	0.5
		Max	33.38	66.13	2411.33	0.83	0.58	2.60	0.75	0.70	0.37	0.70	0.59	Venetian blinds	0.5
A3	*Best solution*		*26.67*	*54.44*	*2095.62*	*0.83*	*0.58*	*1.37*	*0.31*	*0.23*	*0.32*	*0.25*	*0.20*	*Venetian blinds*	*0.5*
	Recommended value range	Min	26.21	53.23	2091.54	0.53	0.37	1.37	0.31	0.20	0.22	0.20	0.20	No shading	0.5
		Max	26.88	55.24	2412.14	0.83	0.58	1.40	0.37	0.54	0.50	0.50	0.61	Venetian blinds	0.5
B1	*Best solution*		*28.17*	*60.48*	*2221.61*	*0.65*	*0.58*	*1.37*	*0.31*	*0.36*	*0.20*	*0.30*	*0.32*	*Venetian blinds*	*0.5*
	Recommended value range	Min	27.67	59.27	2117.89	0.53	0.42	1.37	0.31	0.21	0.20	0.20	0.20	No shading	0.5
		Max	28.84	62.50	2514.84	0.83	0.58	1.80	0.57	0.43	0.26	0.54	0.60	Venetian blinds	0.5
B2	*Best solution*		*25.12*	*62.90*	*2300.58*	*0.53*	*0.58*	*1.37*	*0.31*	*0.45*	*0.20*	*0.44*	*0.39*	*Venetian blinds*	*0.5*
	Recommended value range	Min	24.82	62.10	2075.51	0.45	0.48	1.37	0.31	0.20	0.20	0.20	0.20	No shading	0.5
		Max	25.41	66.53	2465.89	0.83	0.58	1.40	0.37	0.58	0.33	0.64	0.45	Venetian blinds	0.5
C1	*Best solution*		*20.65*	*66.13*	*2074.37*	*0.65*	*0.58*	*2.20*	*0.63*	*0.39*	*0.30*	*0.45*	*0.32*	*Venetian blinds*	*0.5*
	Recommended value range	Min	20.13	64.52	1983.15	0.45	0.42	1.37	0.31	0.25	0.20	0.31	0.21	Venetian blinds	0.5
		Max	21.10	68.95	2545.29	0.83	0.58	2.60	0.75	0.52	0.55	0.61	0.56	Venetian blinds	0.5
C2	*Best solution*		*20.39*	*52.42*	*2103.57*	*0.65*	*0.58*	*1.40*	*0.37*	*0.20*	*0.20*	*0.39*	*0.23*	*Venetian blinds*	*0.5*
	Recommended value range	Min	20.14	50.40	1988.20	0.53	0.48	1.37	0.31	0.20	0.20	0.23	0.20	No shading	0.5
		Max	21.11	54.84	2404.58	0.83	0.58	2.60	0.75	0.58	0.38	0.65	0.70	Venetian blinds	0.5

4 Case study

4.1 Description of the case-study building

An office building in Shanghai in the A2 climate sub-zone was selected as the case-study building (Figure 15). The research team was involved in the design, construction, and operation management of the case building. The cost-effective passive design solution for the case office building in the A2 climate sub-zone proposed in Table 11 was applied during the design phase. In order to evaluate the effectiveness of the design solutions proposed in this paper, the energy consumption for HVAC and indoor thermal parameters is monitored during the operational phase of the case-study building. Meanwhile, subjective evaluation information on occupants' thermal comfort is collected.

The project is located in Changning District, Shanghai. The main function rooms are offices and conference rooms. It is a three-story office building with a floor area of 2866.2 m^2. The height of the building is 14.9m. The window-wall ratio of the building is 0.21 to the east, 0.29 to the west, 0.29 to the south and 0.27 to the north. An external view of the building is shown in Figure 15.

The U-values of the exterior wall and roof are 0.51W/($m^2 \cdot K$) and 0.40W/($m^2 \cdot K$), respectively. Triple glazing (5 low-E +9A+5+9Ar+5) is used in this building. The U-value of an exterior window is 1.5W/ $m^2 \cdot K$, the solar heat gain coefficient (SHGC) is 0.38, and the airtightness level of the exterior window is grade 8, which means the infiltration rate is about 0.5 h^{-1}. The COP and EER for heating and cooling of the VRV system are 3.10 and 3.2, respectively. The main parameters meet the value range requirements of solutions proposed in this paper for the A2 climate sub-zone.

Figure 15: External view of the case-study building : a) Architectural Rendering; b) Photo

To collect the thermal comfort evaluation information of the occupants, a subjective questionnaire survey on indoor comfort in winter and summer was conducted. The subjective survey mainly included occupants' overall satisfaction with the indoor thermal environment, indoor thermal sensation, indoor air humidity sensation, indoor air freshness, and expectations of the indoor thermal environment. The occupants are the staff in the office building.

The survey was conducted from March 4th to 8th, 2019. A total of 78 valid questionnaires were received. During the research period, the average outdoor temperature was 11.8℃, the average indoor temperature was 22.6℃, and the average indoor carbon dioxide concentration was 683PPM. The age, gender, and floor distribution characteristics of the respondents are shown in Table 12. Among them, men accounted for 52.6% and women 47.4%. People who worked on the first floor accounted for 26.9% of the respondents, on the second floor for 46.2%, and on the third floor for 26.9%. The proportion of respondents aged between 20 and 40 is the highest, accounting for 87.2% whilst the proportion of respondents aged between 40 and 50 is lowest at 11.5%.

The summer survey was conducted from August 5th to 9th, 2019. A total of 101 valid questionnaires were received. During the survey period, the average outdoor temperature was 33.2℃, the average indoor temperature was 25.1℃, and the average indoor carbon dioxide concentration was 621 PPM. The age, gender, and floor distribution characteristics of the respondents are shown in Table 12. Among them, men accounted for 46.5% and women 53.5%. The first floor accounted for 26.7% of respondents, the second floor accounted for 56.4% and the third floor accounted for 16.8%. The proportion of respondents aged between 20 and 40 is the highest, accounting for 93.1% whilst the proportion of respondents aged between 40 and 50 is lowest at 6.9%.

Table 12: The age, gender, and floor distribution characteristics of the respondents in winter and summer

Item	**Description**	**Proportion**	
		Winter	Summer
Gender	Male	52.6%	46.5%
	Female	47.4%	53.5%
Age	20~30Y	44.9%	50.5%
	30~40Y	42.3%	42.6%
	40~50Y	11.5%	6.9%
Floor	1^{st}	26.9%	26.7%
	2^{nd}	46.2%	56.4%
	3^{rd}	26.9%	16.8%

4.2 The incremental cost analysis

The initial investment cost is one of the most important factors influencing the developer's decisions and is one of the most important indicators to determine whether the technology solution can be promoted on a large scale. To analyze the cost of the cost-effective building solution, the initial investment cost and incremental cost of the energy-saving technology measures were calculated based on the actual investment of the case-study project. Compared with the base building, the incremental cost of the cost-effective case-study building is 570 CNY/m^2, mainly due to the provision of high-performance exterior windows and shading. The incremental cost of exterior windows and shading was 471.0 CNY/m^2, accounting for 82.6% of the total incremental cost. The incremental costs of the case-study project were reduced by 38.4% compared to the average incremental costs of typical Nearly Zero Energy Buildings in China [50], which is more acceptable to property developers.

4.3 Monitored data analysis

Analyzing the monthly energy consumption of air-conditioning systems ($EUI_{H\&C}$) in 2018 and 2019, the annual $EUI_{H\&C}$ in 2018 was 35.6kWh/ m^2, and in 2019 it was 33.6kWh/ m^2. As shown in Figure 16, the monthly $EUI_{H\&C}$ trend over the past two years is consistent. The cooling energy consumption is mainly concentrated in July and August, and the heating energy consumption is mainly concentrated in January and February. The $EUI_{H\&C}$ in 2018 was higher than that in 2019. The main reason was that the air-conditioning operation strategy in 2019 was optimized based on the previous year's operating experience, which reduced air-conditioning energy consumption.

As stated in Section 2.1.5, the thermal performance of the envelope and other passive design measures are in accordance with the best solution of the A2 climate sub-zone proposed in this paper. The simulated $EUI_{H\&C}$ of the best solution for the A2 sub climate zone is 32.9 kWh/ m^2 (Table 11), which is 2% different from the measured $EUI_{H\&C}$ for the case-study building in 2019, indicating that the occupants' behavior is well-set and the simulation model is well-calibrated.

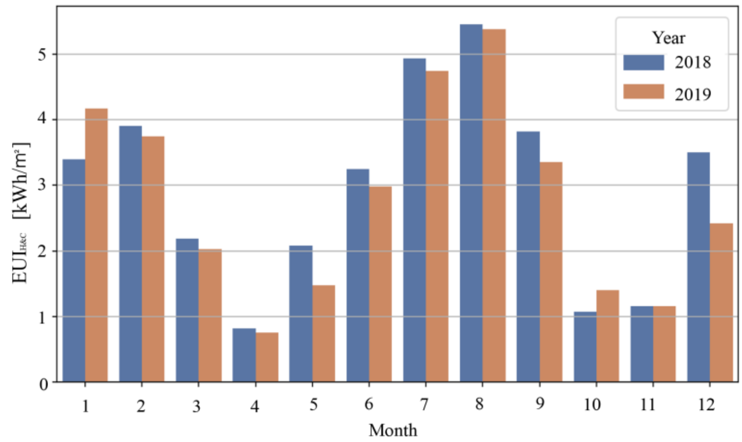

Figure 16: Monthly energy consumption of HVAC in 2018 and 2019

Analyzing the monthly indoor air temperature during working hours (8:00~18:00) in 2018 and 2019, it can be seen from Figure 17 that the fluctuation range of indoor temperature in 2019 is smaller and more stable than that in 2018. The indoor air temperature in winter is maintained at 22.5℃ to 23.5℃, the indoor air temperature during the working period of the transitional season is maintained at 23.5℃ to 25℃, and the indoor air temperature in summer is mostly maintained at 25.5℃ to 26℃. According to GB 50185-2015, the heating setpoint in winter is 20℃ and the cooling setpoint in summer is 26℃. Throughout the year, the indoor temperature is within the comfort range for more than 91.7% of the time and the comfort level indoors was higher in winter, exceeding the heating setpoint by 2.5℃~3.5℃.

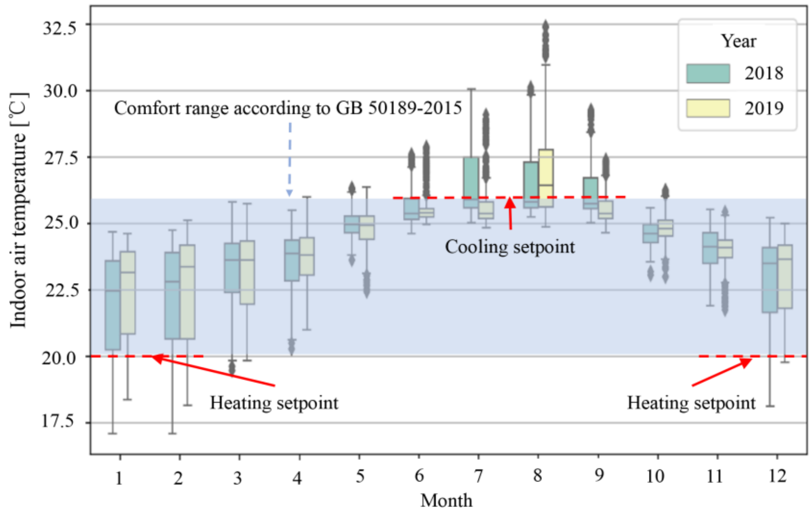

Figure 17: Monthly indoor air temperature during working hours

4.4 Subjective survey data analysis

Figure 18 shows the results of occupant satisfaction with the indoor thermal environment in winter. From the figure, we can see that, in winter, the overall satisfaction is 91.7% (a); 83.3% of occupants wish to maintain the current temperature (b); 50.1% reported feeling uncomfortably dry (c), and 33.3% reported needing more fresh air (d).

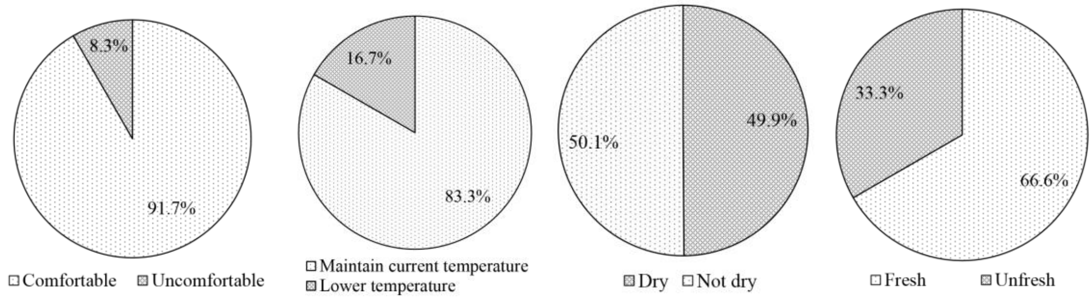

a) The overall satisfaction b) Expected indoor temperature c) Humidity sensation d) Fresh air sensation

Figure 18: Survey results of indoor environment satisfaction in winter

Figure 19 shows the results of occupant satisfaction with the indoor thermal environment in summer. From the figure, we can see that the overall satisfaction in summer is 93.3% (a); 6.7% expect the temperature to be lower, 26.6% expect a higher temperature and the majority of occupants wish to maintain the current situation (b); 20.0% reported feeling dry (c) and only 6.7% reported needing more fresh air (d).

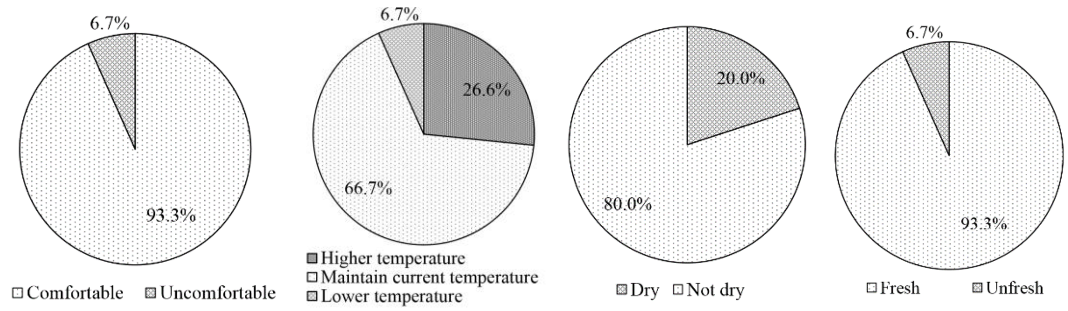

a) The overall satisfaction b) Expected indoor temperature c) Humidity sensation d) Fresh air sensation

Figure 19: Survey results of indoor environment satisfaction in summer

The comfort demand of different occupants for the same environment varies greatly, but a well-created environment should be one that can satisfy more than 90% of the occupants' thermal comfort demands. From the survey results of personal satisfaction with the indoor environment, although most people are satisfied with the indoor temperature, there remains considerable potential to improve the indoor comfort level and reduce energy consumption.

In terms of indoor temperature control, monitoring data shows that the indoor air temperature is maintained at 22.5℃ to 23.5℃ in winter, which is 2.5℃ to 3.5℃ higher than the comfortable indoor temperature limit according to GB50189-2015. The survey results also reflect the phenomenon of overheating in winter and overcooling in summer, with 16.7% of occupants in winter thinking that the indoor thermal environment is too hot and 26.6% of occupants in summer thinking that the indoor thermal environment is too cold. This inevitably leads to some unnecessary energy consumption and adjusting the heating and cooling setpoints are recommended. In terms of humidity control, some humidification measures are needed in both summer and winter. In terms of fresh air control, the indoor air quality can be improved by increasing the appropriate volume of fresh air in summer.

5 Discussion

In general, architects are the end users of optimal building design methods, not the inventors of new technologies or methods [51]. In a building's early design stage, architects often do not have sufficient time to perform complex optimization calculations. This study provides a suggestion for standards by proposing recommended ranges for passive design factors in different sub-climate zones through optimization and decision-making processes. The newly-built office buildings in this area can simply refer to the values directly when determining the design parameters, instead of going through such a complex optimization design process. As demonstrated in the case building, the developed optimal solutions provided to the designers performed well in terms of achieving building energy efficiency, indoor thermal comfort, and cost effectiveness.

It is worthy of note that the designers selected the high thermal comfort level required by the client. The optimization analysis is only based on the discussion of the level I comfort zone. In addition, as the purpose of this study focuses on the optimization of passive design solutions in the early design stage of buildings, the different HVAC system types and energy use modes are not considered. However, the performance of HVAC systems and occupants' behavior significantly impact on the building's operational building energy consumption [52, 53]. Figure 20 illustrates the interactions between $EUI_{H\&C}$, building energy efficiency improvement and occupant comfort demand. As seen in Figure 20, after conducting the decision-making processes proposed in this paper, building performance is improved from grade 3 to grade 2, and the $EUI_{H\&C}$ is reduced from E3 to E2. If the active improvement measures are taken in the subsequent study, i.e., the performance of HVAC systems is improved, the $EUI_{H\&C}$ will be reduced to E1. All the above analyses are based on comfort level I. If occupants adjust their acceptable comfort range, such as by means of clothing adjustment, the $EUI_{H\&C}$ of different building performance grades will be much lower, which will be E3', E2' and E1' respectively.

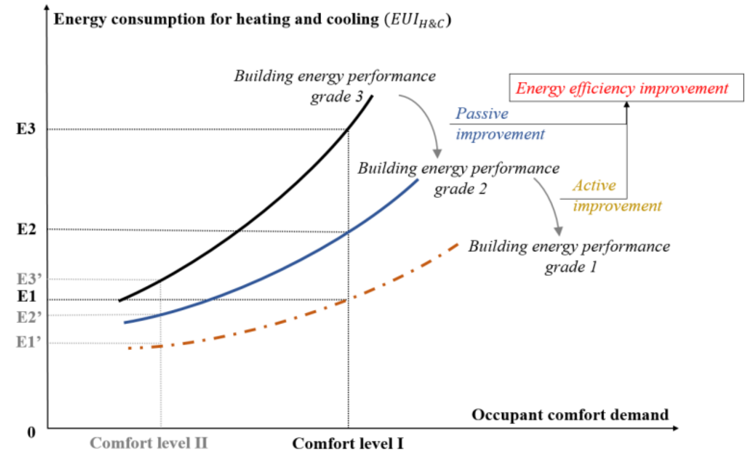

Figure 20: Interactions of energy consumption, building design and occupant comfort demand

In summary, for a real cost-effective building, decision-making for passive design solutions is essential in the early design stage, while in the operation phase, the occupants' comfort needs should be investigated and appropriate HVAC operation strategies implemented. Through climate-responsive passive design and occupant-responsive operation strategies, an optimal balance between building energy consumption and indoor occupant thermal comfort can finally be achieved.

6 Conclusions

This paper proposes a novel three-stage decision-making process for passive design solutions for office buildings in the HSCW zone to achieve energy efficiency, thermal comfort, and cost-effectiveness. This is defined as the reference building identification stage, the sensitivity analysis stage, and the decision-making stage. The advantage of this process is its capacity to support decision-makers in trading-off the goals of energy, comfort, and cost among hundreds of design solutions and rank the alternative options to find the best one. Consequently, the strategy of 'low in energy consumption; high in thermal comfort-balanced economy' can be identified for new office building design in the HSCW zone in China.

A case study of an office building in Shanghai demonstrates the feasibility of the decision-making process. The post-occupant evaluation survey shows the overall satisfaction with the design solution. The proposed method can be implemented in any other region and country. The main conclusions are as follows:

1）It is necessary to identify the reference building for the targeted study area which most reflects the locality and ensures the simulation results are accurate and representative.

2) Sensitivity analysis can help to identify the key factors affecting energy consumption specifically relating to the local climate. The Morris global sensitivity method is applied to calculate the sensitivity indexes of each design variable considering the effect of the interaction between variables on the model output results. The program code of the complicated sensitivity analysis process is developed on the Python platform. In this study, for the total heating and cooling energy demand of an office building in the HSCW climate zone, the top 10 design factors are identified as infiltration rate, U-value of the roof, SHGC of the window, U-value of the wall, south window-to-wall ratio, west window-to-wall ratio, east window-to-wall ratio, U-value of the window, north window-to-wall ratio, and south-facing shading.

3) The results of multi-objective optimization and multi-criteria decision-making show that the optimal design solution can significantly reduce the annual energy consumption for heating and cooling and reduce the percentage of thermal discomfort hours with a small increase in economic costs. Illustrated as an average for each city, compared to the base solution, the best solutions in each city consume 18.7% less energy, reduce occupant discomfort time by 14.0%, but increase costs by 385.54 CNY/m^2.

4）Via a two-year monitoring of the indoor thermal environment and energy consumption of an office building in the A2 climate sub-zone, one of seven climate sub-zones in the HSCW zone with high cooling demand and medium heating demand, it has been demonstrated that the technical solution proposed in this paper can provide a comfortable indoor thermal environment for office buildings while keeping the annual heating and cooling energy consumption within a low range. In terms of energy, the measured $EUI_{H\&C}$ for this office building was 33.6 kWh/ m^2 in 2019, which is only 2% different from the $EUI_{H\&C}$ predicted by the simulation model proposed in this research, indicating that the simulation model is well-calibrated. In terms of comfort, both the monitoring data and the questionnaire study showed that the indoor environment of this case-study building was within the comfort zone throughout the year. In terms of cost, the incremental cost of the case-study building was 570 CNY/m^2, which was reduced by 38.4% compared to Nearly Zero Energy

Buildings in China and is more acceptable to a property developer. The study demonstrates that the decision-making model established in this paper is appropriate, and the proposed design solution for office buildings in the HSCW zone achieves the desired objectives in terms of energy, comfort, and cost, and provides a feasible cost-effective solution.

5) The actual indoor air temperatures in real operation could be higher than the design temperature thanks to the improvement in building performance. Sensing and intelligent control technologies are recommended in the operation stage to avoid overheating of buildings which could cause unnecessary energy waste.

The proposed model in this paper has greatly reduced the number of simulation scenarios through a three-step approach of NSGA-II optimization and decision-making process. Nevertheless, to ensure a high level of accuracy the dynamic simulation of energy consumption is inevitable, which is the most time-consuming part of the model. However, the database generated based on this proposed method can be used for developing a fast energy prediction model using machine learning techniques in future studies.

Acknowledgement

The research is jointly sponsored by the 13th Five-Year Plan National Key R&D Programme "Solutions to Heating and Cooling of Buildings in the Yangtze River Region (SSHCool)" [Grant No: 2016YFC0700301] in association with the UK-China collaborative research project "Low carbon climate-responsive Heating and Cooling of Cities (LoHCool)" funded by the Natural Science Foundation of China [NSFC Grant No. 51561135002] and the UK Engineering and Physical Sciences Research Council [EPSRC Grant No. EP/N009797/1].

References

[1] Building Energy Research Center of Tsinghua University, 2020 annual report on China building energy efficiency, in, Beijing, 2020.

[2] Y. Jiang, D. Yan, S. Guo, S. Hu, China Building Energy Use 2018, Beijing, 2018.

[3] N. Shabrin, S. Bin, S.B.A. Kashem, N. Azreen, T. Ying, Investment and construction cost analysis on net-zero energy building technology, Proceedings of 94 th The IIER International Conference, Bangladesh, 2017.

[4] I. Illankoon, V. Tam, K.N. Le, Cost considerations of green buildings, Life-Cycle Cost Models for Green Buildings, (2021) 45-57.

[5] H. Liu, Y. Wu, B. Li, Y. Cheng, R. Yao, Seasonal variation of thermal sensations in residential buildings in the Hot Summer and Cold Winter zone of China, Energy and Buildings, 140 (2017) 9-18.

[6] Report on Energy Consumption of Public Buildings of Shanghai 2019 (in Chinese), in, http://www.shjzjn.org/SysCommService//Web/uploadfile/APPmaterialfiles/20200722/202007220404017661780.pdf, 2019.

[7] W. Zhu, M. Gong, Z. Wang, H. Chen, Analysis of energy consumption of local administration office buildings in Hangzhou (in Chinese), Architectural Journal, Z2 (2009) 16-19.

[8] J. Yu, C. Yang, L. Tian, D. Liao, A study on optimum insulation thicknesses of external walls in hot summer and cold winter zone of China, Applied Energy, 86 (11) (2009) 2520-2529.

[9] L. Derradji, K. Imessad, M. Amara, F. Boudali Errebai, A study on residential energy requirement and the effect of the glazing on the optimum insulation thickness, Applied Thermal Engineering, 112 (2017) 975-985.

[10] P. Zhu, V. Huckemann, M.N. Fisch, The optimum thickness and energy saving potential of external wall insulation in different climate zones of China, Procedia Engineering, 21 (2011) 608-616.

[11] X. Liu, Y. Chen, H. Ge, P. Fazio, G. Chen, Determination of Optimum Insulation Thickness of Exterior Wall with Moisture Transfer in Hot Summer and Cold Winter Zone of China, Procedia Engineering, 121 (2015) 1008-1015.

[12] A. Ghosh, S. Neogi, Effect of fenestration geometrical factors on building energy consumption and performance evaluation of a new external solar shading device in warm and humid climatic condition, Solar Energy, 169 (2018) 94-104.

[13] C. Marino, A. Nucara, M. Pietrafesa, Does window-to-wall ratio have a significant effect on the energy consumption of buildings? A parametric analysis in Italian climate conditions, Journal of Building Engineering, 13 (2017) 169-183.

[14] J.-W. Lee, H.-J. Jung, J.-Y. Park, J. Lee, Y. Yoon, Optimization of building window system in Asian regions by analyzing solar heat gain and daylighting elements, Renewable energy, 50 (2013) 522-531.

[15] A. Dutta, A. Samanta, S. Neogi, Influence of orientation and the impact of external window shading on building thermal performance in tropical climate, Energy and Buildings, 139 (2017) 680-689.

[16] L. Mottet, J. Song, A. Short C., S. Chen, J. Wu, W. Yu, J. Xiong, Q. Zhang, J. Ge, M. Liu, R. Yao, B. Li, The hot summer-cold winter region in China: Challenges in the low carbon adaptation of residential slab buildings to enhance comfort, Energy and Buildings, 223 (2020) 110181.

[17] Y. Gao, D. Shi, R. Levinson, R. Guo, C. Lin, J. Ge, Thermal performance and energy savings of white and sedum-tray garden roof: A case study in a Chongqing office building, Energy and Buildings,

156 (2017) 343-359.

[18] R. Yao, V. Costanzo, X. Li, Q. Zhang, B. Li, The effect of passive measures on thermal comfort and energy conservation. A case study of the hot summer and cold winter climate in the Yangtze River region, Journal of Building Engineering, 15 (2018) 298-310.

[19] J. Ge, J. Wu, S. Chen, J. Wu, Energy efficiency optimization strategies for university research buildings with hot summer and cold winter climate of China based on the adaptive thermal comfort, Journal of Building Engineering, 18 (2018) 321-330.

[20] F. Kheiri, A review on optimization methods applied in energy-efficient building geometry and envelope design, Renewable and Sustainable Energy Reviews, 92 (2018) 897-920.

[21] Y. Bichiou, M. Krarti, Optimization of envelope and HVAC systems selection for residential buildings, Energy and Buildings, 43 (12) (2011) 3373-3382.

[22] P.A. Deb K , Agarwal S , et al., A fast and elitist multiobjective genetic algorithm: NSGA-II, IEEE Transactions on Evolutionary Computation, 6(2) (2002).

[23] D. Gossard, B. Lartigue, F. Thellier, Multi-objective optimization of a building envelope for thermal performance using genetic algorithms and artificial neural network, Energy and Buildings, 67 (2013) 253-260.

[24] S. Carlucci, G. Cattarin, F. Causone, L. Pagliano, Multi-objective optimization of a nearly zero-energy building based on thermal and visual discomfort minimization using a non-dominated sorting genetic algorithm (NSGA-II), Energy and Buildings, 104 (2015) 378-394.

[25] S. Gou, V.M. Nik, J.-L. Scartezzini, Q. Zhao, Z. Li, Passive design optimization of newly-built residential buildings in Shanghai for improving indoor thermal comfort while reducing building energy demand, Energy and Buildings, 169 (2018) 484-506.

[26] W. Yu, B. Li, H. Jia, M. Zhang, D. Wang, Application of multi-objective genetic algorithm to optimize energy efficiency and thermal comfort in building design, Energy and Buildings, 88 (2015) 135-143.

[27] J. Zhao, Y. Du, Multi-objective optimization design for windows and shading configuration considering energy consumption and thermal comfort: A case study for office building in different climatic regions of China, Solar Energy, 206 (2020) 997-1017.

[28] H.M. Taleb, Natural ventilation as energy efficient solution for achieving low-energy houses in Dubai, Energy and Buildings, 99 (2015) 284-291.

[29] K.W. Chen, P. Janssen, A. Schlueter, Multi-objective optimisation of building form, envelope and cooling system for improved building energy performance, Automation in Construction, 94 (2018) 449-457.

[30] C. Yun, H. Li, Z.R. Yue, J.X. Sheng, Study on Energy-Efficient Retrofit of Public Buildings in Ningbo City, in, 2013.

[31] J. Xiong, R. Yao, S. Grimmond, Q. Zhang, B. Li, A hierarchical climatic zoning method for energy efficient building design applied in the region with diverse climate characteristics, Energy and Buildings, 186 (2019) 355-367.

[32] G. Ledesma, O. Pons-Valladares, J. Nikolic, Real-reference buildings for urban energy modelling: A multistage validation and diversification approach, Building and Environment, 203 (2021) 108058.

[33] M.H. Kristensen, S. Petersen, Choosing the appropriate sensitivity analysis method for building energy model-based investigations, Energy and Buildings, 130 (2016) 166-176.

[34] M. Morris, Factorial Sampling Plans for Preliminary Computational Experiments,

Technometrics, 33:2 (1991) 161-174.

[35] E. Borgonovo, E. Plischke, Sensitivity analysis: A review of recent advances, European Journal of Operational Research, 248 (3) (2016) 869-887.

[36] F. Campolongo, J. Cariboni, A. Saltelli, W. Schoutens, Enhancing the Morris method, in: Sensitivity Analysis of Model Output. Proceedings of the 4th International Conference on Sensitivity Analysis of Model Output (SAMO 2004), 2005, pp. 369-379.

[37] D.M. King, B. Perera, Morris method of sensitivity analysis applied to assess the importance of input variables on urban water supply yield–A case study, Journal of hydrology, 477 (2013) 17-32.

[38] S. Bambrook, A.B. Sproul, D. Jacob, Design optimisation for a low energy home in Sydney, Energy and Buildings, 43 (7) (2011) 1702-1711.

[39] E. Rodrigues, M.S. Fernandes, Overheating risk in Mediterranean residential buildings: Comparison of current and future climate scenarios, Applied Energy, 259 (2020) 114110.

[40] R. Wang, S. Lu, W. Feng, A three-stage optimization methodology for envelope design of passive house considering energy demand, thermal comfort and cost, Energy, 192 (2020) 116723.

[41] U.S. Department of Energy, EnergyPlus Version 8.7 Documentation: Input Output Reference, 2016 (Septemper 30,2016), in, 2016.

[42] X. Li, R. Yao, Q. Li, Y. Ding, B. Li, An object-oriented energy benchmark for the evaluation of the office building stock, Utilities Policy, 51 (2018) 1-11.

[43] L. Enshen, C. Jinhua, Are the annual relative variation rates of energy consumption approximate in different cities with the same shading coefficient?, Building and Environment, 40 (4) (2005) 507-515.

[44] X. Cao, R. Yao, C. Ding, N. Zhou, J. Yao, W. Yu, Q. Xu, L. Pan, B. Li, Energy-quota-based integrated solutions for heating and cooling of residential buildings in the Hot Summer and Cold Winter zone in China, Energy and Buildings, 236 (2021) 110767.

[45] R. Yao, B. Li, J. Liu, A theoretical adaptive model of thermal comfort – Adaptive Predicted MeanVote(aPMV) Building and Environment, 44 (2009) 2089-2096.

[46] N. Delgarm, B. Sajadi, S. Delgarm, Multi-objective optimization of building energy performance and indoor thermal comfort: A new method using artificial bee colony (ABC), Energy and Buildings, 131 (2016) 42-53.

[47] N. Mao, M. Song, D. Pan, S. Deng, Comparative studies on using RSM and TOPSIS methods to optimize residential air conditioning systems, Energy, 144 (2018) 98-109.

[48] S. Hoffmann, E.S. Lee, A. McNeil, L. Fernandes, D. Vidanovic, A. Thanachareonkit, Balancing daylight, glare, and energy-efficiency goals: An evaluation of exterior coplanar shading systems using complex fenestration modeling tools, Energy and Buildings, 112 (2016) 279-298.

[49] A. Kirimtat, B.K. Koyunbaba, I. Chatzikonstantinou, S. Sariyildiz, Review of simulation modeling for shading devices in buildings, Renewable and Sustainable Energy Reviews, 53 (2016) 23-49.

[50] C. Gao, m. Chen, Z. Yu, L. Peng, Technical and economic analysis of Nearly Zero Energy Public Buildings in cold zone (in Chinese), Building Science, 35 (10) (2019) 72-78,181.

[51] X. Shi, Z. Tian, W. Chen, B. Si, X. Jin, A review on building energy efficient design optimization rom the perspective of architects, Renewable and Sustainable Energy Reviews, 65 (2016) 872-884.

[52] H. Sha, P. Xu, Z. Yang, Y. Chen, J. Tang, Overview of computational intelligence for building energy system design, Renewable and Sustainable Energy Reviews, 108 (2019) 76-90.

[53] S. Hu, D. Yan, E. Azar, F. Guo, A systematic review of occupant behavior in building energy policy, Building and Environment, 175 (2020) 106807.